Drosophila APC2 and APC1 Have Overlapping Roles in the Larval Brain Despite Their Distinct Intracellular Localizations

Kathryn Akong,* **Brooke M. McCartney,**†,‡ **and Mark Peifer*,**†,‡,[1]

Curriculum in Genetics and Molecular Biology, †Lineberger Comprehensive Cancer Center, and ‡Department of Biology, University of North Carolina, Chapel Hill, North Carolina 27599-3280

The tumor suppressor APC and its homologs, first identified for a role in colon cancer, negatively regulate Wnt signaling in both oncogenesis and normal development, and play Wnt-independent roles in cytoskeletal regulation. Both *Drosophila* and mammals have two APC family members. We further explored the functions of the *Drosophila* APCs using the larval brain as a model. We found that both proteins are expressed in the brain. APC2 has a highly dynamic, asymmetric localization through the larval neuroblast cell cycle relative to known mediators of embryonic neuroblast asymmetric divisions. Adherens junction proteins also are asymmetrically localized in neuroblasts. In addition they accumulate with APC2 and APC1 in nerves formed by axons of the progeny of each neuroblast-ganglion mother cell cluster. APC2 and APC1 localize to very different places when expressed in the larval brain: APC2 localizes to the cell cortex and APC1 to centrosomes and microtubules. Despite this, they play redundant roles in the brain; while each single mutant is normal, the zygotic double mutant has severely reduced numbers of larval neuroblasts. Our experiments suggest that this does not result from misregulation of Wg signaling, and thus may involve the cytoskeletal or adhesive roles of APC proteins. © 2002 Elsevier Science (USA)

Key Words: APC; β-catenin; Armadillo; brain; Wingless; *Drosophila*; tumor suppressor; neuroblast; cadherin; asymmetric division.

INTRODUCTION

The tumor suppressor APC is mutated in familial adenomatous polyposis, a genetic predisposition to colon cancer. APC is also mutated in >70% of sporadic cases of colon cancer (reviewed in Polakis, 2000). The initial cloning of APC provided few clues as to its normal cell biological function, as it had no obvious relationship to any known protein. The breakthrough came from experiments that revealed that APC physically associates with β-catenin (βcat). βcat and its fly homolog Armadillo (Arm) were known to play two important roles in normal cells, as components of cell–cell adhesive junctions and as key transducers of Wnt signal transduction.

Further experiments revealed that APC is a negative regulator of Wnt signaling (reviewed in Polakis, 2000). APC

is a key component of a multiprotein complex that targets Arm/βcat for phosphorylation by the kinase glycogen synthase kinase 3 (GSK3)/Zeste white 3 (Zw3), leading to its ubiquitination and destruction by the proteasome. Wnt signaling inactivates the destruction complex, allowing Arm/βcat to accumulate and act with its DNA-binding partner TCF/LEF to activate Wnt target genes. In tumors, loss of APC allows constitutive elevation of βcat levels and thus continuous activation of Wnt target genes, which triggers proliferation in that tissue.

In addition to regulating Arm/βcat levels and thus transcriptional activation, APC family members also regulate the cytoskeleton. The first hint of this came from the localization and biochemical properties of human APC. APC binds and bundles microtubules *in vitro*, and when overexpressed, colocalizes with microtubules (Munemitsu *et al.,* 1994; Smith *et al.,* 1994; Zumbrunn *et al.,* 2001). Endogenous APC localizes to the cell cortex, often at sites where bundles of microtubules terminate (Näthke *et al.,*
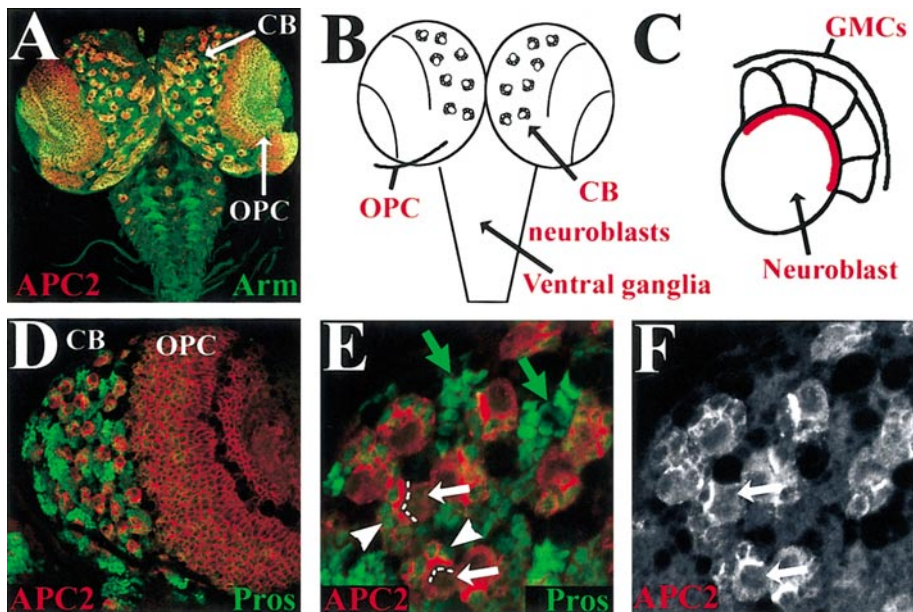

FIG. 1. APC2 accumulates asymmetrically in larval neuroblasts. (A) Double-labeled third instar brain: APC2 (red), Arm (green). (B) Schematic showing the central brain (CB) neuroblasts, outer proliferation center (OPC), and ventral ganglia. (C) Schematic illustrating a neuroblast and its ganglion mother cell (GMC) progeny. The red crescent illustrates the localization of APC2. (D–F) Double-labeled brains: APC2 (D, E, red; F), Pros (D, E, green). (D) Brain lobe. (E, F) Close-up of the CB. APC2 localizes to crescents (dashed lines) where neuroblasts (white arrows) touch GMCs (arrowheads). Pros is found at low levels in GMCs (E, arrowheads) and higher levels in ganglion cells (E, green arrows), but is not found in neuroblast nuclei (E, white arrows).

1996), and an APC–GFP fusion (Mimori-Kiyosue *et al.,* 2000) travels along microtubules to their plus ends and then forms cortical puncta. In contrast, *Drosophila* APC2 colocalizes with cortical actin in a wide variety of tissues (McCartney *et al.,* 1999; Townsley and Bienz, 2000; Yu and Bienz, 1999).

Functional studies subsequently revealed roles for APC family members as Wnt-independent cytoskeletal regulators. In *Drosophila*, APC2 is required for effective tethering of the mitotic spindle to the cortex, acting with Arm in this process (McCartney *et al.,* 2001). This prompted the hypothesis that it may help link the plus ends of astral microtubules to actin at the cortex. In cultured mammalian cells, APC localizes to kinetochores, and in the absence of functional APC, the fidelity of chromosome segregation is reduced (Fodde *et al.,* 2001; Kaplan *et al.,* 2001). Here, APC may help link the plus ends of spindle microtubules to chromosomes. Finally, APC2 plays a role in maintaining the cell–cell adherens junction complex in epithelial cells (Townsley and Bienz, 2000; Hamada and Bienz, 2002).

These roles for APC proteins in both Wnt signaling and Wnt-independent cytoskeletal regulation raises the possibility that APC proteins may mediate known effects of Wnt signaling on the cytoskeleton. Wnt signaling regulates the actin cytoskeleton during the establishment of planar cell polarity, a process whereby epithelial tissues polarize their cytoskeletons along organ or body axes. This influences

processes as diverse as wing hair positioning and dorsal closure in *Drosophila* and convergent extension during vertebrate gastrulation (reviewed in McEwen and Peifer, 2000). Wnt signaling also regulates the positioning of the mitotic spindle in certain cells undergoing asymmetric cell divisions (Gho and Schweisguth, 1998; Rocheleau *et al.,* 1997; Thorpe *et al.,* 1997), and in at least some cases, this effect is direct, without a transcriptional intermediate (Schlesinger *et al.,* 1999).

We examined possible redundancy between APC family members and possible cytoskeletal roles, using the *Drosophila* larval brain as a model (Figs. 1A and 1B). In the brain, neural stem cells known as neuroblasts undergo a series of asymmetric divisions during larval development (Fig. 1C; Ceron *et al.,* 2001; Ito and Hotta, 1992). Each division produces a large daughter that remains a stem cell and a smaller daughter that becomes a ganglion mother cell (GMC), whose subsequent divisions produce neurons. In embryonic neuroblasts, the actin and microtubule cytoskeletons play important roles in the asymmetric localization of neural determinants and in asymmetric division. We previously found that APC2 and Arm localize asymmetrically in larval neuroblasts, accumulating at high levels on the side of the neuroblast where the daughter will be born (Figs. 1C–1F; McCartney *et al.,* 1999).

Here, we present an examination of the localization and function of APC family members in the larval brain. This
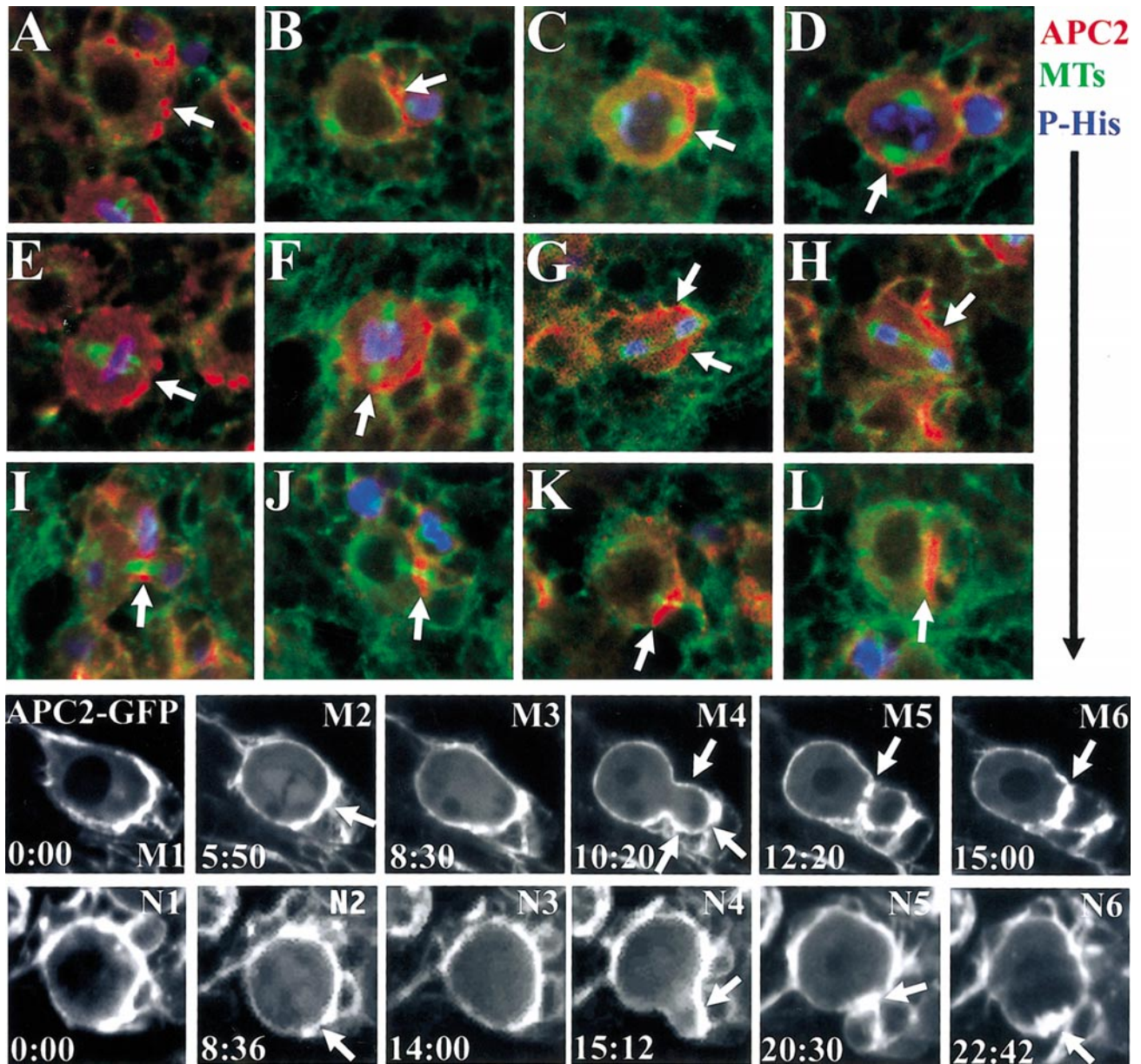
FIG. 2. APC2 accumulation during the cell cycle. (A–L) Triple-labeled third instar CB neuroblasts: APC2 (red), β-tubulin (green), mitotic chromosomes (anti-phosphohistone H3; blue). (A, B) Interphase. Arrows, APC2 crescent. (C, D) Prophase. (E, F) Metaphase. Arrows, spindle pole. (G, H) Anaphase. Arrows, APC2 accumulation on budding GMC daughter. (C, E, G) Divisions in which one spindle pole points toward the center of the APC2 crescent. (D, F, H) Divisions in which one spindle pole points toward the edge of the APC2 crescent. (I–K) Early to late telophase. (L) Neuroblast after cytokinesis. Arrows, APC2 accumulation at cleavage furrow and division site. (M, N) Stills from movies following APC2–GFP during mitosis (M, Movie 1; N, Movie 2). Times in minutes are indicated. (M) Neuroblast in which one spindle pole points toward the center of the APC2 crescent. M2 arrow, spindle pole. M4 arrows, APC2 accumulation all around the budding GMC. M5 and M6 arrows, APC2 accumulation at cleavage furrow. (N) Neuroblast in which one spindle pole points toward the edge of the APC2 crescent. N2 arrow, spindle pole. N4 arrow, APC2 accumulation along one side of budding GMC. N5 and N6 arrow, APC2 at cleavage furrow and division site.

revealed a dynamic localization of APC2 during the neuroblast cell cycle, relative to other neuroblast markers. We found that APC1 also accumulates at low levels in neuroblasts. Neither single mutant had noticeable effects on brain development or neuroblast asymmetric divisions. However, *APC2 APC1* double mutants have substantial

defects in brain development, suggesting functional redundancy between the two APCs. Our data suggest that this role may be Wnt-independent.

MATERIALS AND METHODS

Genetic and Phenotypic Analysis

Alleles used were: $APC2^{\Delta S}$ (McCartney et al., 1999), $APC2^{d40}$ (McCartney et al., 2001), and $APC1^{Q8}$ (Ahmed et al., 1998). $APC2^{g10}$ and $APC2^{f90}$ were generated in an EMS mutagenesis screen, identified by failure to complement $APC2^{\Delta S}$ (unpublished data). Double mutant APC2 APC1 chromosomes were generated by meiotic recombination. All stocks were kept at 25°C. Embryo first and second instar larvae collections were done at 27°C. Wandering third instar larvae collections were done at 25°C. Transgenic lines used for misexpression and overexpression studies were UAS–APC2–GFP (R. Rosin-Arbesfeld and M. Bienz), UAS-APC1 (E. Wieschaus), and UAS–Arm^{S10} (Pai et al., 1997). Transgenes were expressed in specific tissues by crossing to Prospero–GAL4 (Ohshiro et al., 2000) at 27°C. Canton S was the wild type, except when protein levels were compared by immunofluorescence, where controls were histone–GFP transgenics (R. Saint).

Immunolocalization and Time-Lapse Microscopy

Larval tissues were dissected in Schneider's Drosophila Medium (GIBCO) with 10% fetal bovine serum. Brains were fixed for 20 min in 4% paraformaldehyde or 3.7% formaldehyde in PBS/0.2% Triton X-100 with indistinguishable results. Embryos were fixed in 1:1 3.7% formaldehyde in PBS:heptane for 20 min. All were blocked in 1% normal goat serum/0.1% Triton X-100 in PBS for at least 2 h. Primary antibodies were as follows: rat polyclonal anti-APC2 (1:1000), mouse monoclonals anti-Arm N27A1 (DSHB, 1:200), anti-βtubulin E7 (DSHB, 1:500), anti-Prospero (DSHB, 1:4), anti-BP102 (DSHB, 1:100), anti-myc 9E10 (DSHB, 1:100), anti-BrdU (1:100, Becton-Dickinson), rabbit polyclonals anti-Miranda (1:2000, F. Matsuzaki), anti-Bazooka (1:1000, E. Knust), anti-Inscuteable (1:1000, W. Chia), anti-phospho-histone H3 (1:500, Upstate Biotechnology), anti-Armadillo N2 (1:200), and anti-APC1 (1:1000; E. Wieschaus), rat monoclonals anti-DE-cadherin (1:200, M. Takeichi) and anti-α-catenin (1:200, M. Takeichi). For movies, larval brains of genotype UAS–APC2–GFP/Pros–GAL4 were dissected in Schneider's Drosophila Medium with 10% fetal bovine serum and mounted in halocarbon oil (Halocarbon Products) between a glass coverslip and a gas-permeable membrane (Petriperm; Sartorius). Images were collected on a Perkin-Elmer Wallac Ultraview Confocal Imaging System every 6–10 s for 1–2 h.

BrdU Incorporation

Newly hatched first instar larvae were fed Instant Drosophila Medium Blue (Carolina Biological Supply) with 0.5 mg/ml BrdU for 24–28 h at 27°C until the second instar molt.

RESULTS

APC2 Has a Dynamic, Asymmetric Localization during Neuroblast Divisions

We previously found that APC2 localizes asymmetrically in larval neuroblasts (Fig. 1; McCartney et al., 1999). Here,

we extend this observation, examining the dynamic behavior of APC2 during the cell cycle, and comparing its localization with other asymmetric markers and with cytoskeletal and adhesive proteins. We focused our attention on central brain neuroblasts, which are located medially to the proliferation centers of the optic lobes (Figs. 1A and 1B; Ito and Hotta, 1992). Neuroblast divisions are asymmetric in size and fate, with the larger daughter remaining a neuroblast (Figs. 1C, 1E, and 1F, white arrows) and the smaller daughter becoming a ganglion mother cell (GMC; Figs. 1C and 1E, arrowheads; Ceron et al., 2001; Ito and Hotta, 1992). Each central brain neuroblast divides a series of times to produce a "cap" of GMCs (Fig. 1C) that remain joined to the mother, and divide mitotically themselves. Their progeny become ganglion cells and ultimately differentiate as neurons (Fig. 1E, green arrows).

To characterize APC2 dynamic localization during the cell cycle, we took two parallel approaches (Fig. 2; Movies 1 and 2). We used immunofluorescence and confocal microscopy to colocalize APC2, microtubules, and mitotic DNA (via the phosphohistone H3 epitope) in fixed tissue, and we used an APC2–GFP fusion (kindly provided by R. Rosin-Arbesfeld and M. Bienz) under the control of the GAL4–UAS system and driven in a subset of neuroblasts by prospero–GAL4 (pros–GAL4; Ohshiro et al., 2000). The localization of APC2 revealed by these approaches is quite similar, though not identical. APC2–GFP accumulated somewhat more uniformly around the cortical circumference and was present at higher levels in GMCs; we suspect these differences reflect the elevated levels of APC2–GFP, although they could be due to localization differences between the GFP fusion and endogenous APC2. In collecting images, we attempted to select neuroblasts dividing parallel to the plane of focus; however neuroblasts and their GMC daughters are three-dimensional, and neuroblasts do not divide with a defined polarity relative to the brain surface. Thus, we might sometimes have looked at sections not precisely parallel to the plane of division.

During interphase, APC2 forms a strong asymmetric crescent (Fig. 1E, dashed lines; Fig. 2A, arrow), with APC2 accumulating at the border between the neuroblast and its previous daughters; this is where the next daughter will be born. The APC2 crescent remains strong through prophase, as the centrosomes separate and begin to set up the spindle (Figs. 2B–2D, 2M1, and 2N1). The crescent becomes less pronounced at metaphase (Figs. 2E and 2F). The orientation of the neuroblast spindle at metaphase determines where the GMC is born. We observed two different relationships between the cortical APC2 crescent and the mitotic spindle, which in our movies and our confocal images, were present in approximately equal numbers. In about half of the neuroblasts, the forming mitotic spindle was directed toward the center of the APC2 crescent (Figs. 2C, 2E, and 2M2, arrows). In the other neuroblasts, the forming mitotic spindle was directed toward one edge of the crescent (Figs. 2D, 2F, 2N2, arrows). The difference was first apparent during late prophase (Figs. 2B–2D), and continued through

metaphase (Figs. 2E, 2F, 2M2, and 2N2) and anaphase (Figs. 2G, 2H, 2M4, and 2N4). The reason for this difference in APC2 localization in different neuroblasts remains to be determined. One speculative possibility is that the relationship of GMC birth position to the APC2 crescent differs depending on how many GMCs have already been born. We have found that the new GMC daughter is usually born adjacent to one of the earlier daughters (see below). At early stages, when there are relatively few GMC daughters, the spindle may be directed toward the middle of the APC2 crescent. In later divisions, when there are more GMC daughters, the new GMC may be born at the edge of the APC2 crescent, which is found at the interface between the neuroblast and the cap of previous GMC daughters.

As neuroblasts enter anaphase, APC2 remains cortical. In neuroblasts where the spindle pointed toward the center of the APC2 crescent, APC2 surrounds the budding daughter (Figs. 2G and 2M4, arrows). In cells in which the spindle was directed toward the edge of the crescent, APC2 localizes along one side of the GMC (Figs. 2H and 2N4, arrows). As cytokinesis begins, APC2 localizes prominently to the cleavage furrow in all cases (Figs. 2I and 2M5, arrows). This enrichment is even more prominent at the end of cytokinesis (Figs. 2J and 2K, arrows); at times, the cleavage furrow localization resolved into an apparent double ring (Fig. 2N5, arrow). APC2 remains enriched at the division site after cytokinesis, marking the spot where the last daughter was born (Figs. 2L, 2M6, and 2N6, arrows), and it only gradually reexpands to the interface between the neuroblast and all of her GMC daughters.

Our live imaging of APC2–GFP also provided a glimpse of the timing of neuroblast cell cycles. We found that mitosis lasts ~15–20 min. In two cases, we observed a single neuroblast divide twice, allowing us to assess the minimum cell cycle length. In these cases, the two mitoses were completed in 106–120 min. This is comparable to the cell cycle length of embryonic neuroblasts (about 50 min; Foe *et al.,* 1993), and fits previous estimates of neuroblast cell cycle length from BrdU-labeling experiments (e.g., Ito and Hotta, 1992). Other neuroblasts within the same brain, however, divided only once, while still others did not divide at all during the ~2.5 h of the movie.

The Relationship between APC2 Localization and That of Other Asymmetric Proteins

One striking feature of the asymmetric localization of APC2 is that it is present throughout the cell cycle and is particularly strong during interphase. During embryonic neuroblast divisions, most asymmetric markers are only localized during mitosis (reviewed in Jan and Jan, 2001). However, we know less about their localization in larval neuroblasts. We thus examined several asymmetric markers in larval neuroblasts, extending previous work, and compared their localization with that of APC2. In embryonic neuroblasts, the transcription factor Prospero (Pros) and its mRNA are GMC determinants that are asymmetrically localized to the GMC daughter (reviewed in Jan and Jan, 2001). Pros protein then becomes nuclear and helps direct cell fate. In larval neuroblasts, we observed a similar localization. Pros is not detectable in interphase neuroblasts, when the cortical APC2 crescent is strongest (Fig. 1E, dashed line). A small amount of Pros transiently localizes to an asymmetric crescent during mitosis (Fig. 3A, dashed line). Pros is present at low levels in GMC nuclei (Fig. 1E, arrowheads) and at higher levels in the nuclei of ganglion cells (Fig. 1E, green arrows). Our results differ somewhat from those of Ceron *et al.* (2001) who did not detect Pros in GMCs.

We next examined Miranda (Mira), extending the earlier characterization by Ceron *et al.* (2001), and compared Mira with APC2. Mira is basally localized in embryonic neuroblasts, and required there for localization of Pros protein and mRNA (reviewed in Jan and Jan, 2001). We found that, in central brain neuroblasts, Mira is diffusely cytoplasmic during interphase (Fig. 3D), when the APC2 crescent is the strongest. As cells enter mitosis, Mira first becomes cortical (Fig. 3E) and then begins to accumulate asymmetrically on the side of the neuroblast where the daughter will be born (Figs. 3F and 3H, dashed line). By metaphase, Mira asymmetry is very pronounced (Fig. 3I, arrow; Figs. 3J–3L, dashed line). The center of the Mira crescent is always precisely aligned with one spindle pole. As a result, in cells with the spindle pointing toward the center of the APC2 crescent, the Mira and APC2 crescents substantially overlap (Figs. 3F–3H and 3J–3L), while in cells in which the spindle points to the edge of the APC2 crescent, the two crescents are

FIG. 3. The relationship of APC2 to other markers of asymmetric divisions. Third instar CB neuroblasts; in most, the GMC daughter will be born on the right-hand side. (A) Pros (green), mitotic chromosomes (anti-phosphohistone H3; red). Pros accumulates in a transient crescent where the GMC will be born (dashed line). (B–D, F–H, J–L, M, P, S, T) Triple-labeled neuroblasts: APC2 (red), Mira (green), microtubules (blue). (E, I, N, O, Q, R) Double-labeled neuroblasts: Mira (red), microtubules (green). (B–H) Prophase. (I–M) Metaphase. As cells enter prophase, cytoplasmic Mira is recruited uniformly to the cortex (D, E), and then reorganizes into a cortical crescent where the GMC will be born (F, H, dashed line). One spindle pole always points toward the Mira crescent. Arrowhead in (E, F, J): the opposite spindle pole. (F–H, J–L) In cells in which one spindle pole points toward the APC2 crescent, the Mira and APC2 crescents largely overlap (dashed lines). (M) In cells in which one spindle pole points toward the edge of the APC2 crescent, overlap between APC2 and Mira is only partial (red dashed line, APC2; green dashed line, Mira). (N–Q) Anaphase. (R–T) Telophase. Arrowhead, neuroblast. Mira is partitioned into the GMC (N–R, arrows). During anaphase, APC2 brackets the GMC (P), and during telophase it localizes to cleavage furrows (S, T, arrow).
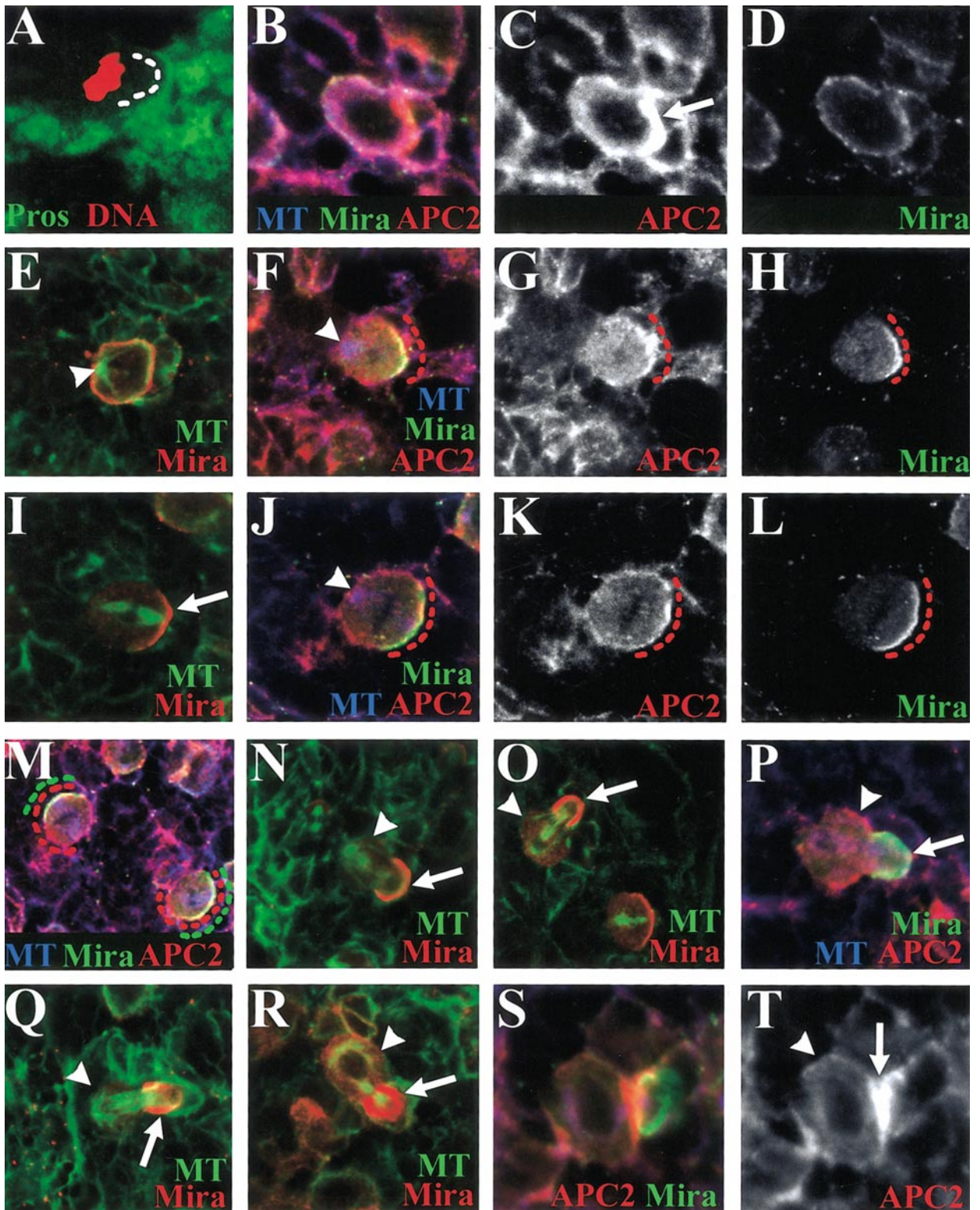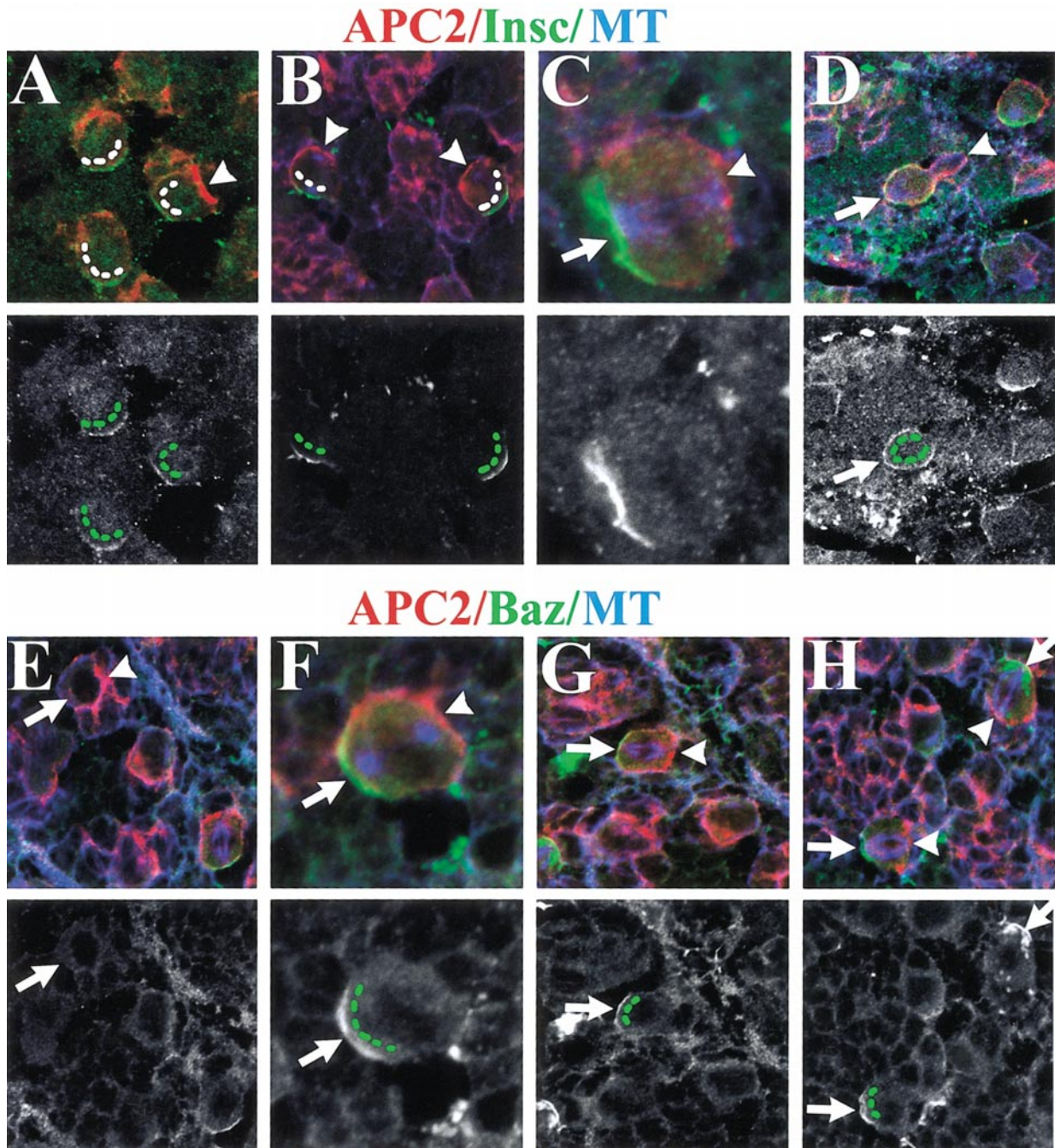
FIG. 4. APC2 localizes opposite Insc and Baz. Third instar CB neuroblasts. (A) Double-labeled: APC2 (red), Insc (green). (B–D) Triple-labeled: APC2 (red), Insc (green), microtubules (blue). Bottom row, Insc alone. (A) Interphase. A prominent APC2 crescent (arrowhead) localizes opposite a faint but detectable Insc crescent (dashed lines). (B) Prophase. The APC2 crescent becomes less pronounced (arrowheads) as the Insc crescent becomes more pronounced (dashed lines). (C) Metaphase. Insc localizes to the cell cortex (arrow) at the end of the spindle opposite where the GMC will be born, thus not overlapping APC2 (arrowhead). (D) Anaphase. Insc localizes to the neuroblast cortex (arrow in top panel, dashed line in bottom panel), while APC2 surrounds the neck of the GMC (arrowhead). (E–H) Triple-labeled: APC2 (red), Baz (green), microtubules (blue). Bottom row, Baz alone. (E) Interphase. In cells with a strong APC2 crescent (arrowhead), Baz is diffusely cytoplasmic (arrow). (F) Prophase. Baz localizes to a crescent at the end of the spindle (top-arrow, bottom-dashed line) opposite where the daughter will be born, and thus does not overlap APC2 (arrowhead). (G) Metaphase. Baz remains in a crescent (top-arrow, bottom-dashed line) opposite APC2 (arrowhead). (H) Anaphase onset. Baz remains localized to the cortex (top-arrow, bottom-dashed line) near the end of the spindle opposite where the daughter will be born and thus opposite APC2 (arrowhead).

offset (Fig. 3M). Mira is partitioned into the GMC during anaphase (Figs. 3N–3R, arrows), while APC2 relocalizes to the cleavage furrow (Figs. 3S and 3T, arrow). Mira could still be detected in some GMCs, which we suspect are those that were recently born (see below).

In contrast to Mira and Pros, Inscuteable (Insc) and Bazooka (Baz) localize to the apical sides of embryonic neuroblasts, where they play essential roles in asymmetric divisions (reviewed in Jan and Jan, 2001). Insc is asymmetrically localized in larval neuroblasts (Parmentier *et al.,* 2000; Ceron *et al.,* 2001). We found that Insc localizes to the side of the neuroblast opposite that of APC2 through much, if not all, of the cell cycle (Figs. 4A–4D, dashed lines and arrows). Interestingly, there is a weak Insc crescent during interphase (Fig. 4A), that became stronger through prophase and metaphase (Figs. 4B and 4C). During anaphase, Insc localized to the neuroblast cortex but not the GMC daughter (Fig. 4D). Baz localization was similar to that of Insc, though no cortical localization during interphase was detected (Fig. 4E, arrow). During prophase and metaphase, Baz localized to a crescent (Figs. 4F and 4G, dashed lines and arrows) opposite APC2 (Figs. 4F and 4G, arrowheads), and as the chromosomes began to separate, Baz localized to a tight cap opposite the future GMC (Fig. 4H). Together, these data confirm that larval and embryonic neuroblasts asymmetrically localize many of the same proteins, and that APC2 localizes on the GMC side of the neuroblast, overlapping Mira and opposite Baz and Insc.

Adherens Junction Proteins Localize Asymmetrically in Larval Neuroblasts

In our initial characterization of APC2, we found that Arm also localizes asymmetrically in neuroblasts (McCartney *et al.,* 1999). We extended this, examining the localization of Arm's adherens junction partners DE-cadherin and α-catenin. When central brain neuroblasts undergo a sequential series of asymmetric divisions, the GMCs remain associated with their neuroblast mother, resulting in a cap of GMCs in association with each neuroblast. APC2 localizes strongly to the boundary between the neuroblast and each GMC, and more weakly to the borders between the GMCs (Figs. 1E and 1F). APC2 is present at lower levels in ganglion cells and differentiating neurons (Figs. 1E and 1F). The adherens junction proteins DE–cadherin, Arm, and α-catenin all show a striking and asymmetric localization pattern in central brain neuroblasts (Figs. 5A–5H). All precisely colocalize both at the boundary between neuroblasts and GMCs (dashed lines) and at the boundaries between GMCs (arrowheads). DE–cadherin, Arm, and α-catenin are also all expressed in epithelial cells of the outer proliferation center (e.g., Fig. 5E, bracket).

The localization of DE–cadherin and the catenins is consistent with the idea that cadherin–catenin-based adhesion could help ensure that GMCs remain associated with each other, via association with their neuroblast mother. To further explore this, we examined how successive

GMCs are positioned relative to their older GMC sisters, using two different approaches. We first used Mira (Fig. 5I, green; Figs. 5K and 5L green) to mark the newborn GMCs (arrowheads) and DE–cadherin (Fig. 5I, red; Figs. 5J and 5L, red) to mark the neuroblast (arrows) and all of her GMC daughters. Mira localizes to a crescent on the side of the neuroblast where the daughter will be born, and then is segregated into the daughter. We found that Mira persists for some time in newborn GMCs, and that it remains detectable in the other GMCs as well (Fig. 5K), thus allowing us to examine the position of newborn GMCs relative to their older sisters. In many cases, new GMCs are clearly born at the edge of the cluster of older GMCs. This is particularly striking in neuroblasts with many progeny (e.g., Fig. 5I, arrows). It is worth noting that the cluster of daughters is three-dimensional, comprising a "cap" of daughters in three dimensions rather than the two-dimensional line of daughters illustrated in Fig. 1. We thus suspect new daughters are born near the edge of this cap. We obtained further resolution by live imaging of dividing neuroblasts in brains expressing APC2–GFP (Movie 3 = M1, Movie 4 = M2). In the two cases when we followed a single neuroblast through two divisions, the orientation of the mitotic spindles were similar in each division, such that second daughter (M1b or M2b) was born very near the first (M1a or M2a).

These data suggest that neuroblasts and their GMC progeny remain closely associated. The GMCs then divide to form ganglion cells and ultimately neurons. Our data further suggest that these latter cells may also remain associated and send their axons together toward targets in the central brain. When we sectioned more deeply into the brain, below each cluster of neuroblasts and GMCs (Fig. 5N, arrowhead; Fig. 5O, arrow and arrowhead), we could detect structures that appear to be axons projecting from these groups of cells (Fig. 5N, arrows; Figs. 5P and 5Q, arrow and arrowheads). These axons label with Arm (Figs. 5N–5Q), DE–cadherin (Fig. 5N), APC2 (Figs. 5O–5Q), and APC1 (see below). Arm also localizes to the axons of the neuropil, while DE–cadherin (Fig. 5N, large arrow) and APC2 (Fig. 5Q, inset, arrow) are present at low levels or are absent from this structure.

APC2 Is Not Essential for Asymmetric Divisions

Given APC2's asymmetric localization and our previous observation that it plays a role in spindle attachment in syncytial embryos (McCartney *et al.,* 2001), we hypothesized that APC2 might play a role in spindle orientation and thus division asymmetry in larval neuroblasts. To test this, we examined neuroblast divisions in larvae homozygous, hemizygous, or trans-heterozygous for different *APC2* alleles. *APC2*$^{\Delta S}$ and *APC2*^{d40} are strong hypomorphic alleles that disrupt cortical localization of APC2 (McCartney *et al.,* 1999, 2001). *APC2*$^{\Delta S}$ results from the deletion of a serine residue in the Arm repeat region, while *APC2*^{d40} encodes a truncated protein lacking much of the Arm-binding region.

$APC2^{g10}$ and $APC2^{f90}$ are stronger alleles, as assessed by their maternal-effect embryonic phenotype (unpublished data). They may be null mutations, as they result from premature stop codons in the Arm repeat region (unpublished data) and thus do not produce a protein detectable with our antibody, which recognizes the C-terminal half of APC2.

All four *APC2* mutations are zygotically viable, suggesting that brain development was unlikely to be severely disrupted. We examined the brains of larvae mutant for three of these alleles, and found that the asymmetric divisions appeared unaffected, as assessed by Mira localization (Figs. 6A and 6B, arrows), its match with spindle position, and the size asymmetry between mother and daughter (Figs. 6A and 6B; data not shown). In the case of $APC2^{\Delta S}$, we also examined Pros, Insc, and Baz, all of which were correctly localized (Fig. 6E, dashed line; Figs. 6F–6H, arrows). Finally, we examined the effect of loss of APC2 function on the levels and localization of Arm, as Arm levels are substantially elevated in embryonic ectodermal cells mutant for *APC2* (McCartney *et al.,* 1999). We saw no differences in either Arm levels or localization in the brains of *APC2* mutant larvae (Figs. 6I–6L). DE–cadherin localization also appeared normal (data not shown). To complete this analysis, we also examined whether a null mutation in the other fly *APC* gene, $APC1^{Q8}$, had any effect on asymmetric divisions. Once again, asymmetric divisions, as assessed by Mira localization (Figs. 6C and 6D, arrows), its match with spindle position, and the size asymmetry of mother and daughter, appeared normal (Figs. 6C and 6D).

APC1 and APC2 Differ in Their Cell Biological Properties

Thus, despite its striking localization, APC2 is not essential for brain development. One possible explanation is that APC1 is also expressed in larval neuroblasts and plays a redundant role there. We thus examined the localization and function of APC1 in brain development. In embryos, APC1 is expressed in primordial germ cells and in CNS axons (Hayashi *et al.,* 1997). We used anti-APC1 antibody to examine its expression in the larval brain, using the null allele $APC1^{Q8}$ (Ahmed *et al.,* 1998) as a negative control. APC1 accumulates at apparently low levels throughout the brain. It is largely diffuse throughout the cell, with slight cortical enrichment (Figs. 7A and 7C). There was a small amount of residual staining in the *APC1* mutant (Figs. 7B and 7D), that we suspected might represent slight cross-reactivity with APC2 (cross-reactivity is detectable in immunoblotting; data not shown). To test this, we stained brains from $APC2^{g10}$ mutants (Figs. 7F and 7H–7J), which lack detectable APC2, with anti-APC1. These brains exhibited only slightly reduced levels of staining compared to wild-type controls (Figs. 7E and 7G; cortical neuroblast staining was slightly reduced), suggesting that any cross-reaction with APC2 was weak. This experiment also highlighted the strong accumulation of APC1 in the axons

emerging from clusters of neuroblast, GMCs, and their progeny (Figs. 7I and 7J, arrows). Together, these data indicate that low levels of APC1 accumulate in neuroblasts, GMCs, and their progeny, with higher levels found in axons projecting from these cells. Thus, APC1 could potentially compensate for loss of APC2 in the larval brain. We explore this further in the next section.

We next compared the cell biological properties of APC1 and APC2. The four known APC family members, two in flies (Hamada *et al.,* 1999; Hayashi *et al.,* 1997; McCartney *et al.,* 1999; Yu *et al.,* 1999) and two in mammals (Groden *et al.,* 1991; Nakagawa *et al.,* 1998; van Es *et al.,* 1999), share certain structural features but differ in others. All share a block of N-terminal Arm repeats, followed by a set of short repeated sequences that serve as binding sites for Arm/βcat and Axin. These regions comprise most of fly APC2, which is the shortest family member. Fly APC1 (Hayashi *et al.,* 1997) is significantly longer at its N and C termini. Its extended C-terminal region contains a sequence similar to the microtubule-binding domain of human APC. Given these structural differences between fly APC1 and APC2, we asked whether they would exhibit similar or distinct cell biological properties when both were expressed at equivalent levels. We used the GAL4–UAS system to overexpress each protein in the same cellular environments, and examined where each localized under these conditions.

We first expressed each protein in the larval brain, using pros–GAL4 (Ohshiro *et al.,* 2000), which drives expression in most but not all neuroblasts, as well as in the outer proliferation center. To determine the level of protein expression driven by pros–GAL4 relative to the levels of the endogenous protein, we drove APC2–GFP with pros–GAL4, visualizing both the endogenous plus the exogenous fusion protein using anti-APC2 antibody. In the same experiment, we stained wild-type brains that did not mis-express APC2. When we imaged these brains at the same confocal settings, we found that pros–GAL4 drives expression at levels substantially above that of the endogenous protein. The endogenous protein in wild-type brains (Fig. 8B) was barely visible at settings where the GAL4-driven protein was easily visible (Fig. 8A). However; when we turned up the brightness setting, we could easily visualize the endogenous protein in the wild-type brain (Fig. 8C). Overexpression with pros–GAL4 of APC2-GFP, APC1, or both had no effects on adult viability or on overall brain morphology.

When we overexpressed APC2–GFP (Figs. 8A and 8D; see also Figs. 2M and 2N), it localized asymmetrically to the cortex of the larval neuroblasts (Figs. 8A and 8D, arrows), as well as to the junctions between the GMCs (Fig. 8D, bracket) and thus paralleled the localization of endogenous APC2 (Fig. 8C, arrow). In contrast, when we overexpressed APC1 (Figs. 8E–8M), it had a strikingly different localization. APC1 localized very strongly to the centrosome and the microtubules emanating from it (Figs. 8E–8M, white arrowheads). It also localized to interphase microtubule arrays in cells of the inner proliferation center (e.g., Figs. 8K
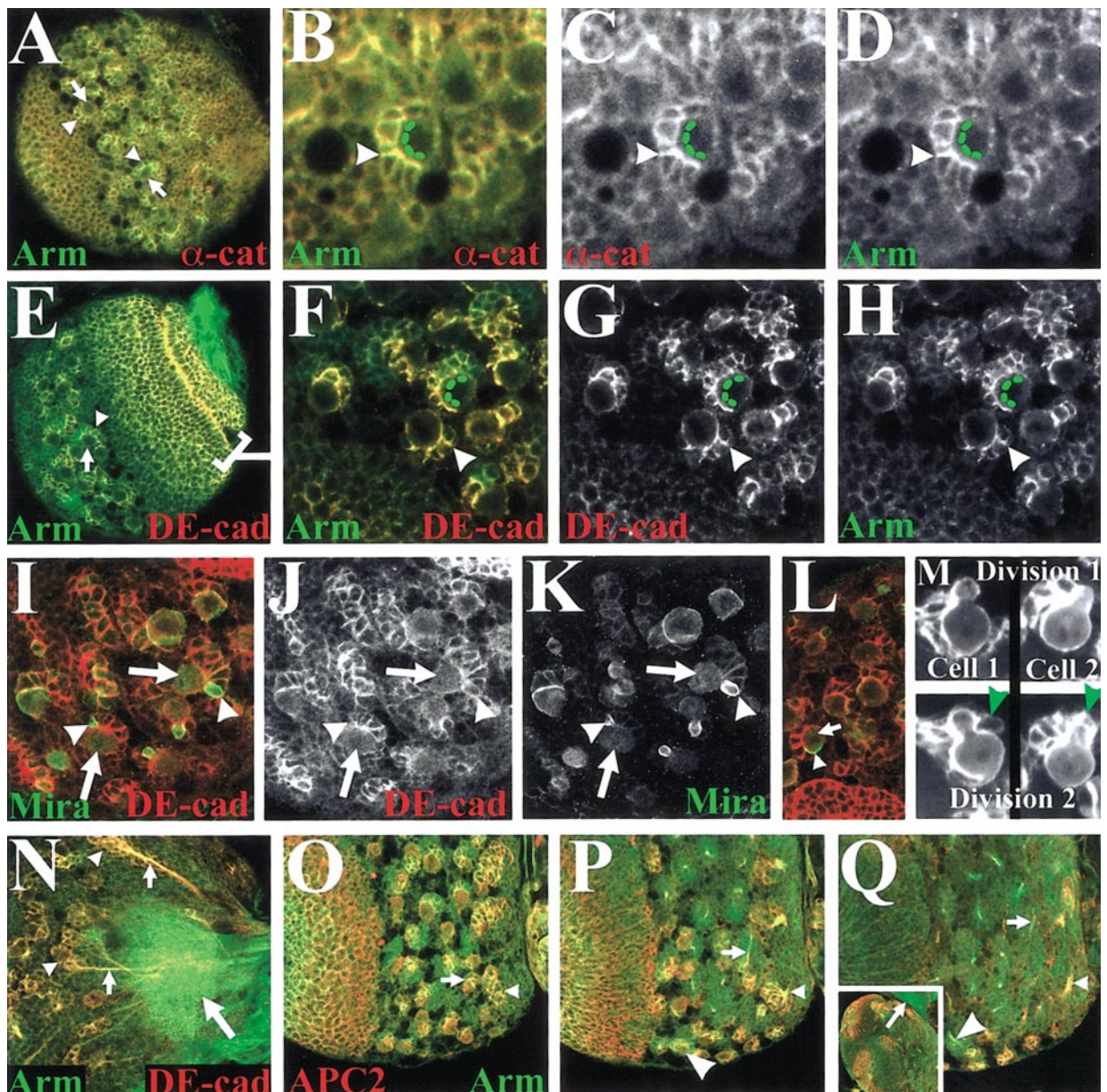
FIG. 5. Adherens junction proteins are asymmetrically localized in neuroblasts. Third instar brains or CB neuroblasts. (A–D) Double-labeled: Arm (green), α-catenin (red). Both precisely colocalize (A). (B–D) They localize to junctions between the neuroblast and the GMCs (dashed line) and junctions between GMCs (arrowhead), and are present at lower levels in ganglion cells. (E–H) Double-labeled: Arm (green), DE–cadherin (red). (E) Both precisely colocalize in most regions of the brain (E), including neuroblast (arrow)–GMC (arrowhead) clusters, and the epithelial cells of the proliferative centers (bracket). (F, H) Close-up showing colocalization to junctions between neuroblast and GMCs (e.g., dashed line) and junctions between GMCs (e.g., arrowhead). (I–L) Double-labeled CB neuroblasts (e.g., arrows): Mira (green), DE–cadherin (red). Mira localizes to a crescent during mitosis, and is concentrated in GMCs, where it remains at detectable levels for some time (K). New GMCs (e.g., I, L, arrowheads) are often born at the edge of the cluster of previous GMCs. (M) Still images from APC2–GFP movies of two different neuroblasts (cell 1 = movie 3; cell 2 = movie 4), which were filmed through two successive mitoses, showing each cell in anaphase of division 1 and division 2. Spindle orientation remained similar for the second division, and thus the second GMC was born near to the spot on the neuroblast cortex where the first GMC was born. Green arrowhead in division 2, approximate location of the earlier daughter. (N–Q) Axons emerging from the progeny of individual neuroblast–GMC clusters accumulate DE–cad, Arm, and APC2. (N) Double-labeled brain: Arm (green), DE–cadherin (red). Arrowheads, two neuroblast/GMC/neuron clusters. Small arrows, two nerves emerging from these clusters, which express both proteins. Large arrow, the neuropil, which is enriched for Arm but not DE-cadherin. (O–Q) Successive sections of double-labeled brain: Arm (green), APC2 (red). Arrowhead, arrow in (O), large arrowhead in (P), neuroblast/GMC clusters. Arrowheads and small arrows in (P) and (Q) follow putative axons emerging from these clusters through successively deeper sections. The neuropil (Q, inset, arrow) is enriched for Arm but not APC2.
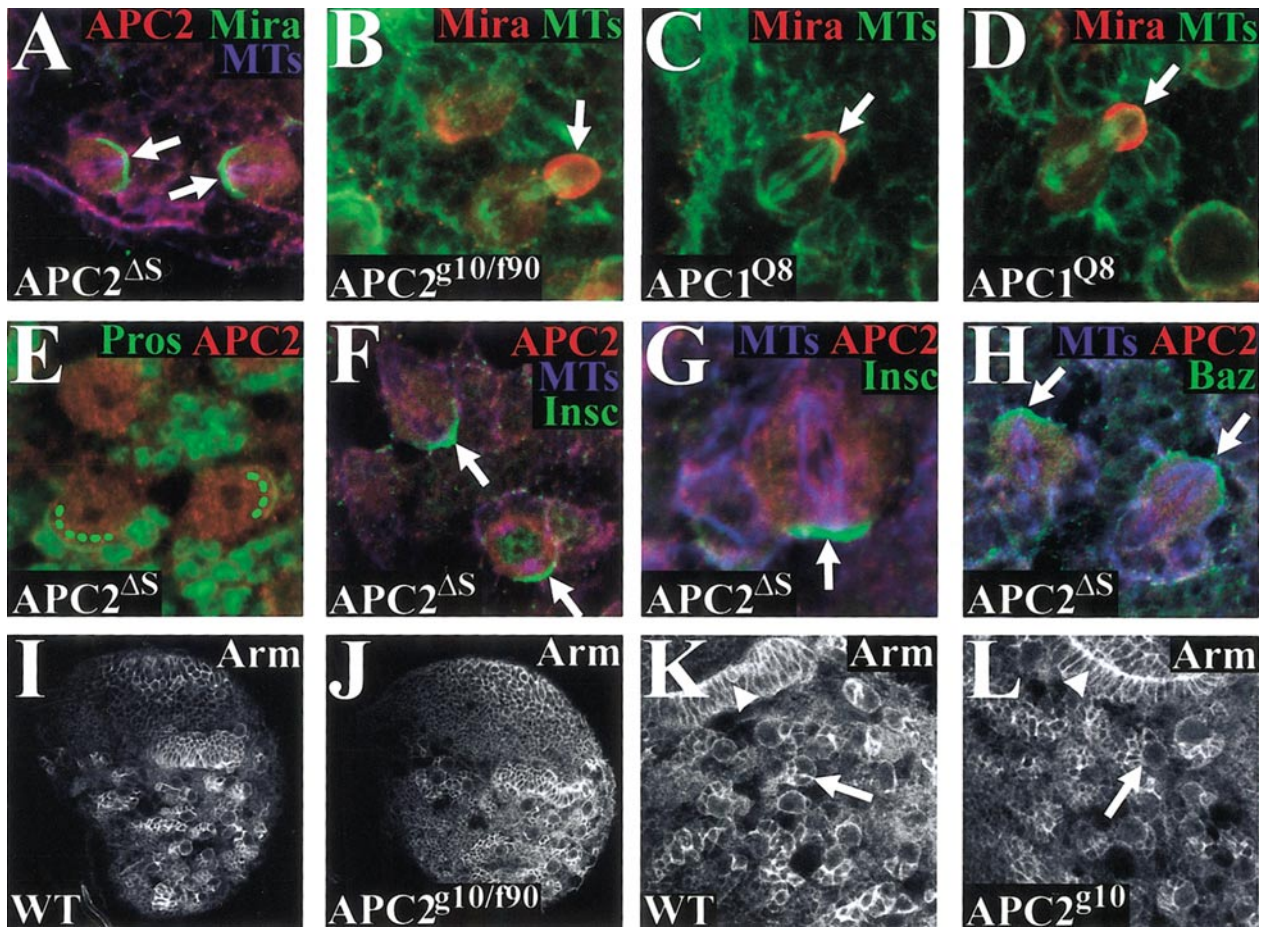
FIG. 6. Asymmetric divisions occur normally in *APC2* and *APC1* single mutants. Third instar brains or CB neuroblasts. (A) Triple-labeled *APC2*$^{\Delta S}$ mutant neuroblasts: APC2 (red), Mira (green), microtubules (blue). Mutant APC2 protein is no longer cortical, but asymmetric Mira localization during metaphase (A, arrows) is normal. (B–D) Double-labeled *APC2*^{g10}/*APC2*^{f90} mutant neuroblasts (B) or *APC1*^{Q8} mutant neuroblasts (C, D): Mira (red), microtubules (green). Mira localization is normal (arrows). (E–H) *APC2*$^{\Delta S}$ mutant neuroblasts. (E) Double-labeled: APC2 (red), Pros (green). Pros accumulates in transient crescents (dashed lines) as in wild-type. (F, G) Triple-labeled: APC2 (red), Insc (green), microtubules (blue). (H) Triple-labeled: APC2 (red), Baz (green), microtubules (blue). Insc and Baz localize normally (arrows). (I–L) Wild-type (identified using histone-GFP) and *APC2*^{g10} mutant brains simultaneously labeled to visualize Arm and imaged under the same confocal conditions. Arm levels and localization were normal in the brain lobes (I, J), the neuroblast–GMC clusters (K, L, arrows) and the epithelial cells of the inner proliferation center (arrowhead).

and 8L, bracket). It did not strongly colocalize with all microtubule-based structures; however, for example, it was only marginally enriched in the spindle at metaphase (Fig. 8K, inset). In parallel, we carried out similar localization experiments after mis-expression in the embryonic epidermis, with similar results; APC2 localizes to the cell cortex, while APC1 localizes to centrosomes and microtubules (see accompanying paper). Together, the data from brains and embryos suggest that sequence differences between APC1 and APC2 direct them to quite different intracellular locations, despite their strong similarity in the core region of the protein.

Mammalian APC protein can oligomerize (Day and Alber, 2000), and we thus wondered whether fly APC1 and APC2 proteins might interact. To begin to examine this, we examined the effect of APC1 overexpression on the localization of endogenous and overexpressed APC2. Pros–GAL4 is not expressed in all neuroblasts (e.g., Figs. 8F and 8G, green arrowheads), allowing cells not overexpressing APC1 to serve as an internal control. Overexpression of APC1 in neuroblasts had a striking effect on APC2: its localization to cortical crescents was substantially diminished in neuroblasts overexpressing APC1 (e.g., Figs. 8F, 8G, and 8K–8M, white arrowheads), but not in those that did not (e.g., Figs. 8F and 8G, green arrowheads; Figs. 8H–8J, white arrow). Further, endogenous APC2 now localized to centrosomes (e.g., Figs. 8F, 8G, and 8K–8M, white arrowheads), though less strikingly than APC1. This suggests that APC1
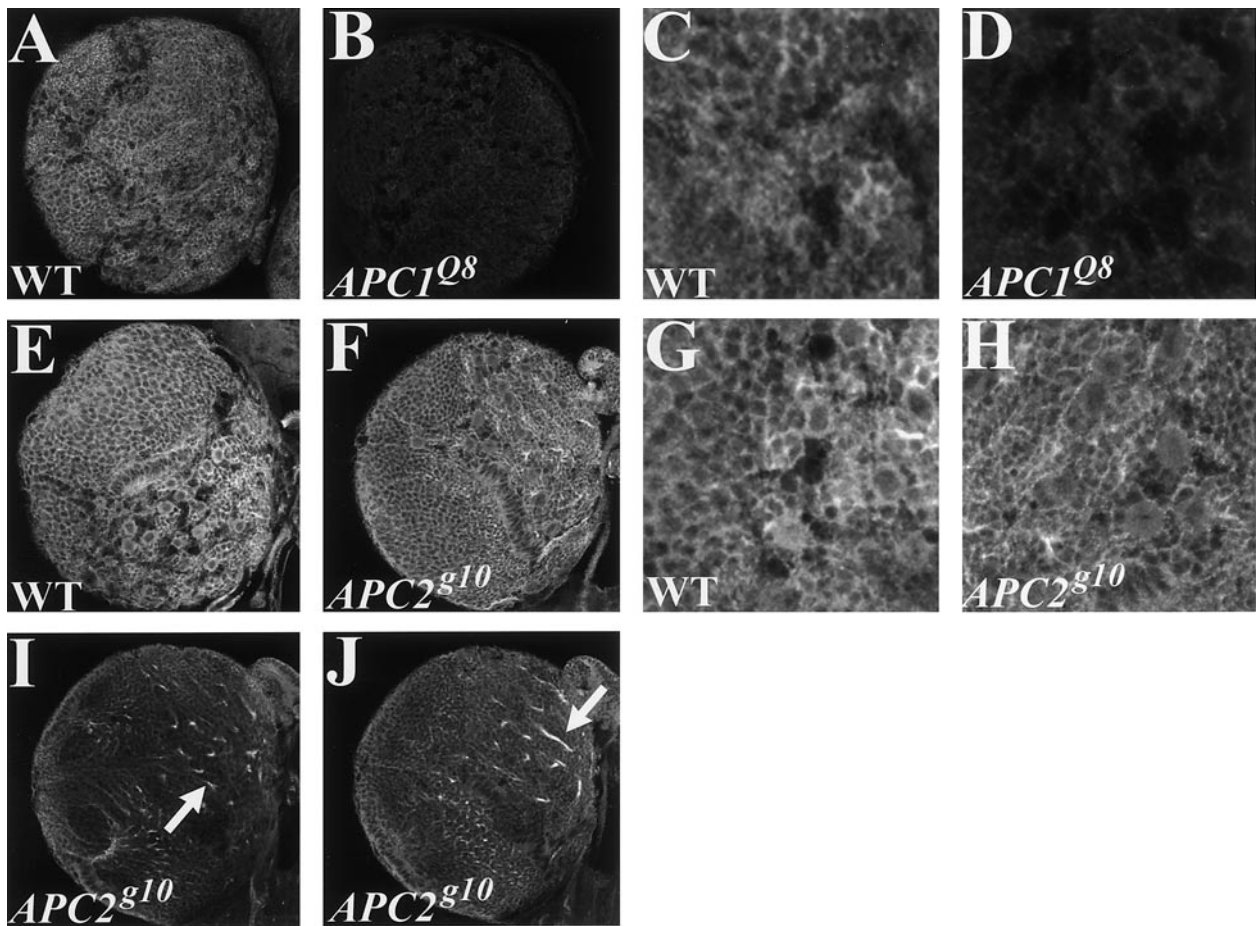
FIG. 7. APC1 localization in the larval brain. Third instar brains stained to reveal APC1. (A–D) Wild-type (A, C, expressing Histone-GFP to allow identification) and *APC1^{Q8}* (protein null) mutant brains labeled and visualized together, to allow comparison of signal level. (E–H) Wild-type (E, G, expressing Histone–GFP to allow identification) and *APC2^{g10}* (null for reactivity with APC2 antibody) mutant brains labeled and visualized together, to allow comparison of signal level. In wild-type, APC1 antibody stains the cytoplasm of all cells in the brain, and is cortically enriched in many cells. The level of labeling is substantially reduced in the *APC1^{Q8}* mutants (A vs B, C vs D), suggesting that the antibody recognizes APC1 specifically. The slight residual cortical staining may reflect slight cross-reaction with APC2, as it was slightly reduced in an *APC2* mutant (G vs H). (I, J) Successive sections through an *APC2^{g10}* mutant brain. APC1 accumulates at high levels in axons emerging from the progeny of neuroblast–GMC clusters (arrows).

and APC2 may interact, either directly or indirectly, allowing APC1 to recruit APC2 to a new location.

We further examined this issue by coexpressing APC1 and APC2–GFP in the same neuroblasts, using Pros–GAL4 to drive both simultaneously (Figs. 8N–8S). When we did so, APC2–GFP localized both to its normal cortical site (e.g., Figs. 8N–8S, green arrowheads) and, more weakly, to centrosomes and microtubules with APC1 (Figs. 8N–8S, white arrowheads). We also looked at the effects of APC2 overexpression on APC1. APC1 localized most prominently to centrosomes and their associated microtubules (e.g., Figs. 8N–8S, white arrowheads), but we now saw APC1 accumulation at the cortex (Figs. 8N–8S, green arrowheads); this was less prominent when APC1 was singly overexpressed (Figs. 8E–8M). These data suggest that APC2 may recruit

APC1 to the cell cortex; however, this is subject to the caveat that the APC1 antibody may weakly cross-react with APC2.

APC1 and APC2 Play Functionally Redundant Roles in Brain Development

Given the striking localization of APC2 in the brain, we were surprised that *APC2* mutants had no apparent brain defects. The brain is only one of several tissues where neither single mutant had any apparent phenotype (Ahmed *et al.,* 1998; McCartney *et al.,* 1999); this was surprising as Wg signaling plays an important role in several of these tissues. The realization that APC1 is also expressed in the brain (Fig. 7) raised the possibility that it might play a

partially redundant role in this tissue. To test this, we examined the phenotype of animals mutant for both *APC1* and *APC2*.

APC1 and *APC2* single mutants are both zygotically viable to adulthood (Ahmed *et al.,* 1998; McCartney *et al.,* 1999). The only known problem in *APC1* mutants are morphological defects and inappropriate apoptosis in the photoreceptors of the eye (Ahmed *et al.,* 1998), while *APC2* zygotic mutants are morphologically wild type, with a phenotype only emerging in embryos maternally and zygotically mutant (McCartney *et al.,* 1999). In contrast, we found that *APC2 APC1* double mutants are zygotically lethal. Two allelic combinations, $APC2^{\Delta S}$ $APC1^{Q8}$ and $APC2^{g10}$ $APC1^{Q8}$, die as second instar larvae, while the third, $APC2^{d40}$ $APC1^{Q8}$, dies primarily during the first larval instar. None of the double mutants had any apparent defects in segment polarity as first instar larvae (data not shown). Mitotic activity during larval stages is restricted to the imaginal tissues and the brain, and imaginal discs are dispensable for larval development. Given this and the observed expression pattern of APC2 and APC1 in the CNS, we examined brain development in double mutant larvae.

During normal brain development, most embryonic neuroblasts exit the cell cycle during late embryogenesis. Immediately after hatching, the only mitotically active neuroblasts are the so-called mushroom-body neuroblasts, which are at a ventrolateral position (Ito and Hotta, 1992). Eight hours after hatching, other neuroblasts become mitotically active, such that by 20 h after hatching, 20–30 central brain neuroblasts per hemisphere are dividing. During the early first instar, the cells of the optic anlage become epithelially arranged and also begin dividing. The number of proliferating neuroblasts continues to increase, plateauing 20–50 h after egg laying.

$APC2^{\Delta S}$ $APC1^{Q8}$ zygotic double mutants die during the second larval instar. We thus compared wild-type and double mutant animals immediately after they completed the second instar larval molt. Double mutant brains were essentially normal in size, and the optic anlage had become epithelial (data not shown). However, double mutants had a strikingly different pattern of neuroblast proliferation than wild type. While presumptive mushroom body neuroblasts continued to proliferate (Figs. 9B, 9D, 9F, and 9H, arrowheads), the number of other mitotic neuroblasts was drastically reduced relative to wild type (Figs. 9A, 9C, 9E, and 9G), as assessed both by phosphohistone H3-labeling (Figs. 9A–9D) and by Mira and Pros staining (Figs. 9E–9I). We saw a similar, though less drastic, block in mitotic activity in $APC2^{g10}$ $APC1^{Q8}$ (Fig. 9I, arrowheads). To determine whether DNA synthesis was initiated but mitosis blocked, we labeled larvae with BrdU throughout the first instar, identifying cells that replicated their DNA during this period. The results were similar to those seen with mitotic markers. $APC2^{\Delta S}$ $APC1^{Q8}$ double mutants had drastically reduced numbers of BrdU-labeled cells; most labeled cells remaining appeared to be mushroom-body neuroblasts (Figs. 9J and 9K, arrowheads). We next examined whether embryonic CNS development was altered, by examining the axonal scaffold produced by progeny of the embryonic neuroblasts, using the marker BP102 that labels all axons (Fig. 9L). Zygotic double mutants were distinguished from wild-type siblings by the presence (Fig. 9N) or absence (Fig. 9O) of APC1 in the CNS. The axonal scaffold was unaltered in $APC2^{\Delta S}$ $APC1^{Q8}$ double mutants (Fig. 9M), suggesting that embryonic neuroblast proliferation is at least roughly normal. Finally, we examined whether we could detect defects in asymmetric divisions in double mutants, as assessed by examining asymmetric localization of Mira. In

---

FIG. 8. APC1 and APC2 localize differently when overexpressed in the larval brain. Third instar brains. (A–D) APC2–GFP localizes to the cortex even when highly overexpressed. (A, B) APC2–GFP is expressed at levels much higher than endogenous APC2. (A) Brain lobes overexpressing UAS–APC2–GFP under control of *pros*–GAL4. (B) Wild-type control brain. (A) and (B) were imaged by using the same confocal settings, visualizing both APC2 and APC2–GFP with anti-APC2. Levels of APC2 expression driven by *pros*–GAL4 (A) are much higher than those of endogenous APC2 (B). (C) Same brain as (B), with brightness turned up to show endogenous APC2. (A, C) Arrows, neuroblast GMC clusters. Brackets, outer proliferation center. (D) APC2–GFP driven by *pros*–GAL4 localizes like endogenous APC2, accumulating in neuroblast cortical crescents (e.g., arrow) and junctions between GMCs (e.g., bracket). APC2–GFP also accumulates in ganglion cells, neurons and their nerves (e.g., arrowheads). (E–M) APC1 overexpressed with *pros*–GAL4 localizes to centrosomes and microtubules, and recruits endogenous APC2 to these structures. (E) APC1 localizes to centrosomes and associated microtubules (white arrowheads; green arrowheads show cells with separated centrosomes), as well as to interphase microtubules in the outer proliferation center (arrow). (F, G) Double-labeled brain lobe: APC1 (F, green), endogenous APC2 (F, red; G). In neuroblasts that do not express APC1, APC2 remains in cortical crescents (green arrowheads). In neuroblasts overexpressing APC1 (white arrowheads), APC1 localizes to centrosomes, while endogenous APC2 cortical localization is reduced and it relocalizes to centrosomes. (H–J) Triple-labeled CB neuroblasts: APC1 (H, green; I), APC2 (H, red), microtubules (H, blue; J). (K–M) Double-labeled CB neuroblasts: APC1 (K, green; L), APC2 (K, red; M). APC1 localizes to centrosomes and microtubules, and endogenous APC2 is recruited into these structures (white arrowheads; H–J green arrowheads, cell with separated centrosomes). In neuroblasts that do not misexpress APC1, APC2 remains cortical (arrows). During metaphase, both APC1 and APC2 weakly label spindles (K, inset). In the outer proliferation center, APC1 accumulates along interphase microtubules (K–M, bracket), while APC1 and APC2 colocalize in cortical spots (K–M, green arrowheads). (N–S) Neuroblasts mis-expressing both APC1 (N, green; P; Q, green; R) and APC2–GFP (N, red; O; Q, red; S) under the control of *pros*–GAL4. APC1 localizes to centrosomes (white arrowheads) and to the cortex (green arrowheads). APC2 strongly labels the cortex (green arrowheads) and localizes more weakly to centrosomes (white arrowheads).
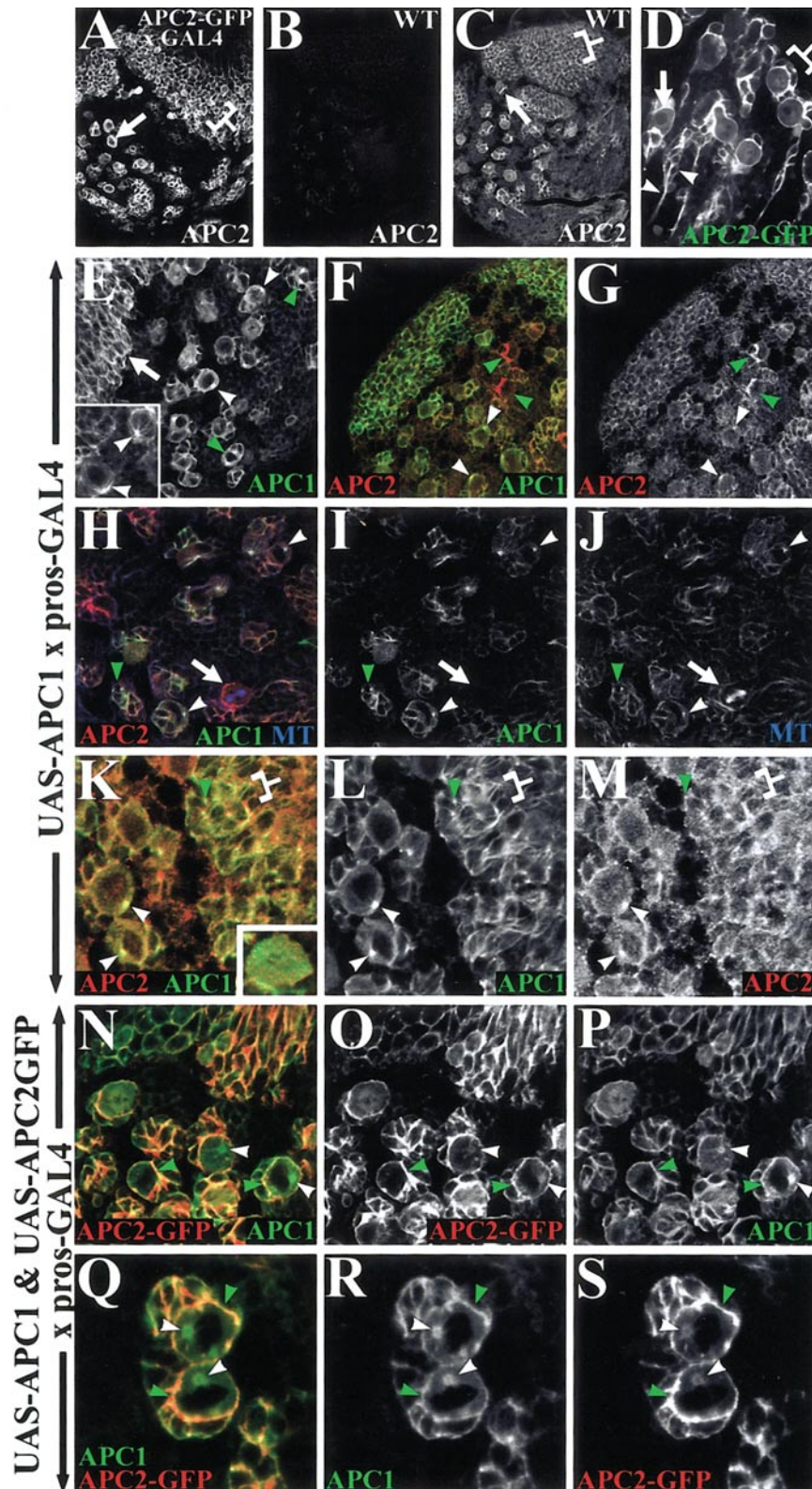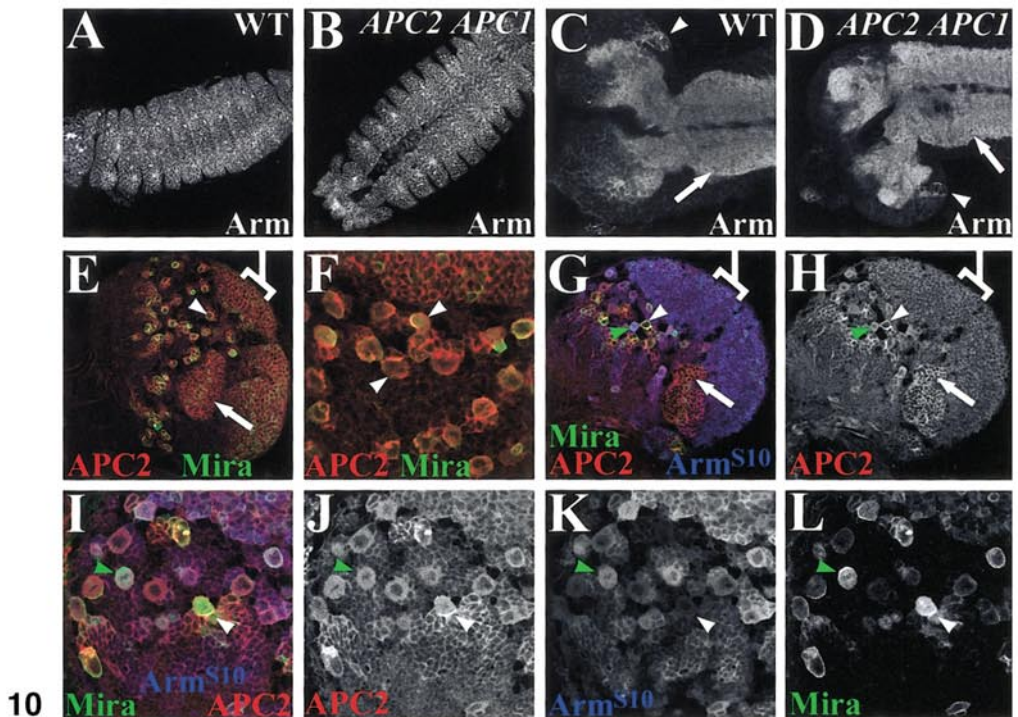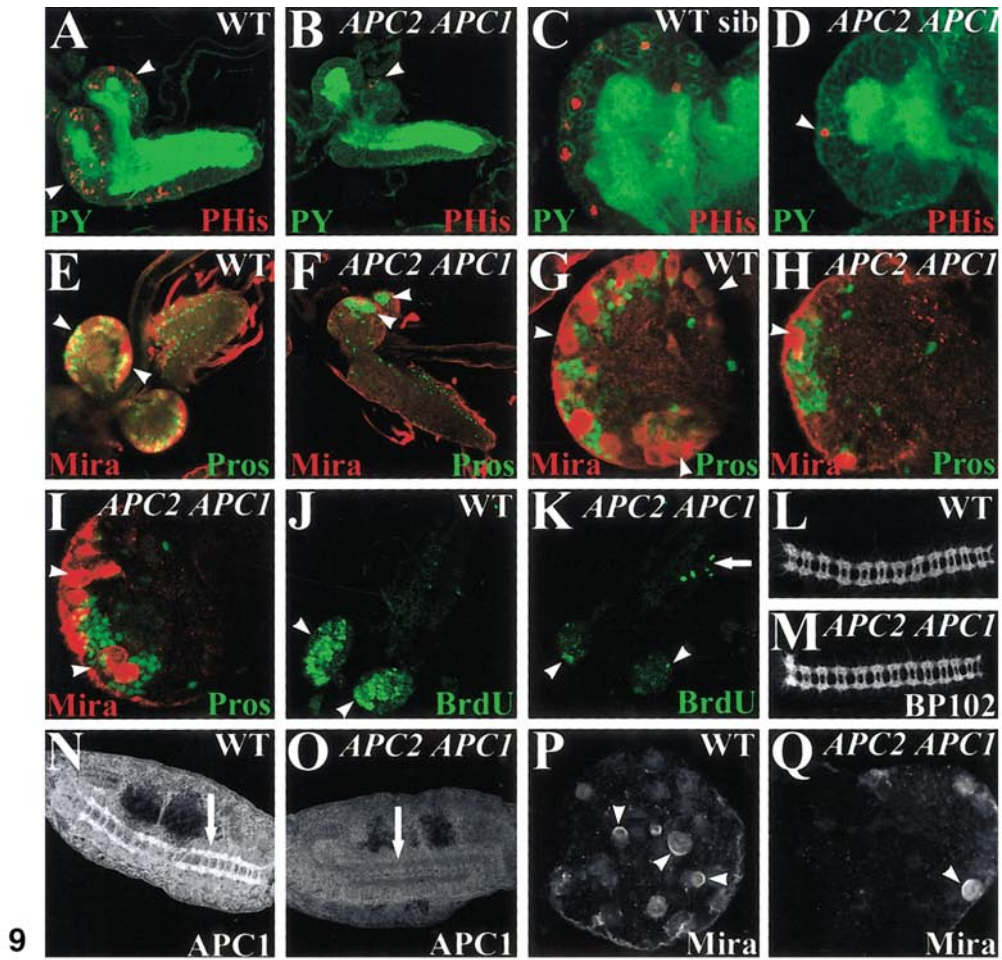
the wild-type first and second instar brain, the localization of Miranda is less strikingly asymmetric, with reasonably high levels in the cytoplasm (Fig. 9G). However, we could detect crescents of Mira and see it localize to smaller daughters (Fig. 9P). In double mutants, many fewer Mira-positive neuroblasts were seen, but we could find neuroblasts with Mira crescents or Mira segregated to smaller daughters (Fig. 9Q). In addition, Prospero-positive daughters are found in the double mutants, though in reduced numbers. These data thus suggest that asymmetric divisions still can occur, though it remains possible that they are not entirely normal or occasionally fail. Together, these data suggest that most likely explanation for the mutant phenotype is that double mutant embryonic neuroblasts do not reenter the cell cycle during the first larval instar.

APC1 and APC2 regulate Wg signaling, and thus one mechanism that could underlie the zygotic double mutant phenotype is the failure to properly regulate Arm levels. To test this, we first examined Arm accumulation in zygotic double mutant embryos. We identified stage 16 double mutants by the absence of APC1 accumulation in the CNS, and examined the level of Arm accumulation relative to wild-type embryos. Arm accumulation appeared completely normal in the epidermis of $APC2^{g10}\ APC1^{Q8}$ double

mutant embryos (Fig. 10B) relative to wild-type controls (Fig. 10A), suggesting that maternally contributed protein from the two loci is sufficient for normal Arm regulation in the embryo.

We next looked at Arm accumulation in the brains of midfirst instar larvae. Figures 10C and 10D display projections of optical sections through the entire brain. In the wild-type brain, Arm accumulates heavily in axons of the ventral nerve cord and neuropil (Fig. 10C, arrow). Arm accumulation in the cellular portion of the first instar brain is much lower. In the brain lobes, we found weak cortical staining of most cells. The only significant Arm accumulation outside the neuropil was in cells that we believe are epithelial cells of the developing optic lobe (Fig. 10C, arrowhead). The accumulation of Arm in zygotic double mutant brains is not substantially elevated from that of wild-type. Arm levels in the neuroblasts and cell bodies are unchanged (Fig. 10D, arrowhead), while Arm levels in axons are similar or only slightly elevated (Fig. 10D, arrow). These data thus do not support the hypothesis that elevated Arm levels cause the phenotype.

As a second test for the hypothesis that the double mutant phenotype results from deregulated Arm levels, we attempted to mimic it by misexpressing in neuroblasts

FIG. 9. *APC2 APC1* double mutants have defects in larval neuroblast proliferation. (A–D) Wild-type (A, C) and $APC2^{\Delta S}\ APC1^{Q8}$ (B, D) double mutant second instar larval brains. Double-labeled: phosphotyrosine (green, marks cell junctions and axons), mitotic cells (red, phosphohistone H3). (A, C) In wild-type brains (A) or brains of wild-type siblings of double mutants (C, identified using a GFP-marked Balancer chromosome), many mitotic neuroblasts (red) are seen in any section through the brain lobes (A, arrowhead). Mitotic cells are found all around the circumference (C). (B, D) In double mutants, the number of mitotic cells is strongly reduced, and those remaining are often in the position of the mushroom-body neuroblasts (arrowheads). (E–I) Wild-type (E, G), $APC2^{\Delta S}\ APC1^{Q8}$ (F, H) double mutant, or $APC2^{g10}\ APC1^{Q8}$ (I) double mutant second instar brains. Double-labeled: Mira (red, labels neuroblasts), and Pros (green, labels GMCs, ganglion cells and neurons). (E, G) Wild-type. Neuroblasts (red) are found all around the circumference of the brain (arrowheads), and they have given rise to many differentiating progeny (green). (F, H, I) Double mutants. The number of neuroblasts (red) and differentiating progeny (green) is reduced, with the most severe reduction in $APC2^{\Delta S}\ APC1^{Q8}$ (E, H). Neuroblasts remaining (arrowheads) are often in the position of the mushroom-body neuroblasts. (J, K) Wild-type (J), and $APC2^{\Delta S}\ APC1^{Q8}$ (K) double mutant second instar brains labeled with BrdU to visualize cells that have replicated their DNA. (J) Wild-type. Many cells in the brain lobes have replicated DNA during the labeling period (arrowheads). (K) Double mutant. The number of labeled cells is substantially reduced (arrowhead). Arrow, polyploid cells from another tissue. (L–O) Stage 15 wild-type (sibling of a double mutant; L, N) and $APC2^{\Delta S}\ APC1^{Q8}$ zygotic double mutant (M, O) embryos. Double-labeled: axonal scaffold (using BP102 antibody; L, M), APC1 (accumulates in axons; N, arrow; O; note lack of APC1). The axonal scaffold appears normal. (P, Q) Wild-type (P) and $APC2^{\Delta S}\ APC1^{Q8}$ double mutant (Q) second instar brains, labeled to visualize Mira. In wild-type neuroblasts of this stage (P), Mira labels both the cytoplasm and accumulates in cortical crescents (arrowheads). While double mutant brains have far fewer Mira-positive neuroblasts (Q), seemingly normal cortical crescents of Mira are detected (arrowhead).

FIG. 10. The *APC2 APC1* double mutant phenotype does not result from elevated Arm levels. (A, B) Epidermal Arm levels in stage 16 $APC2^{g10}\ APC1^{Q8}$ double mutant embryos (B) and wild-type siblings (A) are indistinguishable. Double-labeled to visualize Arm and APC1 (not shown), which we used to distinguish double mutants from wild-type siblings. (C, D) Arm levels in the ventral nerve cord (arrows) and brain lobes (arrowheads) of mid-first instar wild-type (C) or $APC2^{\Delta S}\ APC1^{Q8}$ zygotic double mutants (D) are indistinguishable. Double mutant larvae, identified using a GFP-Balancer, were stained and imaged together with wild-types (marked with Histone–GFP). (C, D) Projections of sections through the entire brain. In both genotypes, high levels of Arm are found in the neuropil—other cells show only weak cortical staining—with somewhat elevated levels in a few cells that we believe are epithelial cells of the developing optic lobes (arrowheads). (E, F) Double-labeled wild-type third instar brains: APC2 (E, F, red), Mira (E, F, green). Arrowheads show neuroblasts with typical cortical APC2, while the bracket and arrow illustrate the cortical localization of APC2 in the cells of the outer and inner proliferation center, respectively. (G–L) Third instar brains in which Arm^{S10} was mis-expressed by using pros–GAL4. Triple-labeled: APC2 (G, I red; H, J), Mira (G, I, green; L), Arm^{S10} (via myc-epitope; G, I, blue; K). The brains are normal in all aspects except one. In neuroblasts expressing Arm^{S10}, APC2 is diffusely cytoplasmic (green arrowheads), while in neuroblasts not expressing Arm^{S10}, APC2 remains cortical (white arrowheads). Cortical APC2 localization is also lost in the outer proliferation center (bracket), that expresses Arm^{S10}, but not in the inner proliferation center (arrow), that does not. Asymmetric divisions are normal.

Arm[S10], a mutant form of Arm that cannot be targeted for destruction (Pai *et al.,* 1997). Mis-expression of Arm[S10] mimics the *APC2* single mutant in the embryonic epidermis (McCartney *et al.,* 1999) and the *APC1* single mutant in the photoreceptors (Ahmed *et al.,* 1998), as both result from deregulated Wg signaling. We thus used Pros-GAL4 to express myc-tagged Arm[S10] in neuroblasts, and verified expression by staining with antibodies to myc. To our surprise, these animals survived larval development and emerged as viable adults, suggesting that deregulation of Arm destruction does not disrupt neuroblast development.

We also examined the consequences of Arm[S10] expression on third instar brains directly to look for more subtle effects on neuroblast proliferation or asymmetric divisions. Animals expressing Arm[S10] had brains of normal morphology, with normal numbers of neuroblasts that were mitotically active and exhibited normal asymmetric cell divisions (Figs. 10E and 10F vs 10G–10L). We did see one striking effect of Arm[S10], however. In neuroblasts expressing Arm[S10], the amount of cortical APC2 was strongly reduced (Figs. 10G–10L, green arrowheads), perhaps because the excess Arm protein in these neuroblasts competed for APC2 binding, preventing it from associating with its cortical binding partners. Neuroblasts not expressing pros–GAL4 were an internal control; they retained normal cortical APC2 (Figs. 10G–10L, white arrowheads). We saw a similar reduction in cortical APC2 in the outer proliferation center (Figs. 10G and 10H, bracket), which expressed Arm[S10], relative to cells of the inner proliferation center (Figs. 10G and 10H, arrow), that did not. Together, these results suggest that the larval brain phenotypes of *APC2 APC1* double mutants do not result from elevated levels of Arm or activation of Wg signaling.

DISCUSSION

APC was first identified because loss-of-function mutations result in colon tumors. In this context, it functions as a negative regulator of Wnt signaling, via its role in the Arm/βcat destruction complex (reviewed in Polakis, 2000). The role in tumors reflects a normal role for APC proteins in Wnt regulation, as demonstrated by the phenotype of loss-of-function mutations in *Drosophila APC1* and *APC2* (Ahmed *et al.,* 1998; McCartney *et al.,* 1999; Yu *et al.,* 1999). However, this relatively simple picture recently became more complex. First, APC proteins have novel abilities that appear separate from their role in the destruction complex. These include interactions with cytoskeletal proteins, by which APC family members influence Wnt-independent cytoskeletal events (see Introduction). Second, both mammals and flies have two APC family members, which share common structural elements but also have structural differences. These new data raise new questions about the functions of APC family members, which we have begun to address with the work presented here.

Possible Roles for APC1 and APC2 in Brain Development

Our data demonstrate that APC1 and APC2 play redundant roles in larval brain development. Further, our data suggest that this role is Wg-independent, as it is not mimicked by elevating Arm levels. This contrasts with what we and others observed in embryos and imaginal discs, where the two proteins also have overlapping functions but where these clearly involve Wg signaling (see accompanying paper; Ahmed *et al.,* 2002). Hamada and Bienz (2002) recently found that APC1 and APC2 also play redundant roles in cell adhesion during oogenesis. Maternal contribution of the two proteins appears sufficient for many if not all aspects of embryogenesis, as double mutant embryos hatch with a normal cuticle pattern and an apparently normal brain. However, we saw striking differences between the larval brains of wild-type and double mutant animals. During wild-type development, most neuroblasts become quiescent during late embryogenesis, with only the mushroom body neuroblasts mitotically active upon hatching (Ito and Hotta, 1992). In the middle of the first instar, however, other embryonic neuroblasts reenter the cell cycle and proliferate. In the *APC2 APC1* double mutant, this appears not to occur, as we see far fewer total neuroblasts, and the number of brain cells in mitosis and the number that have gone through S-phase is substantially reduced.

There are several possible interpretations of these data, which now must be tested. First, double mutant neuroblasts may be driven into apoptosis, as occurs in *APC1* mutant photoreceptors (Ahmed *et al.,* 1998). However, we think this is less likely, as overall brain size is not substantially reduced in the double mutants, and expression of activated Arm in neuroblasts does not mimic the phenotype as it did in the photoreceptors. However, this possibility must now be rigorously tested. Second, it is possible that there are defects in asymmetric cell divisions, which, if they resulted in symmetric divisions producing two GMC daughters, would rapidly deplete the pool of stem cells. We observed Mira crescents in the subset of double mutant neuroblasts that continue to divide, however, suggesting that at least some cells can undergo asymmetric divisions. This does not rule out a more subtle defect in asymmetric divisions; we must further test this by generating clones of double mutant cells in the brain of third instar larvae, when asymmetric divisions are easier to visualize. We think the most likely model is that neuroblasts simply remain quiescent. This could be due to intrinsic problems in reactivating the cell cycle in the brain, or could be due to defects in signaling from other tissues; ecdysone regulates cell cycle reactivation and this influences a similar brain phenotype seen in *trol* mutants (Datta, 1995, 1999). We need to test this possibility by trying to rescue the double mutant phenotype by expressing APC1 or APC2 specifically in the brain.

Regardless of which theory is correct, we must determine the mechanism by which defects arise. Earlier studies

suggested two possibilities. First, loss of both APC proteins may elevate Arm levels, triggering the phenotype by activating a program of gene expression. We did two experiments to test this possibility, both of which suggest that this mechanism is less likely. First, expression of activated Arm in neuroblasts does not disrupt brain development. Second, Arm levels are not substantially elevated in zygotic double mutant embryos or larval brains. Other possible mechanisms are cytoskeletal or adhesive ones. If the two APCs have overlapping functions in cytoskeletal regulation and/or cell adhesion, defects in these might affect cell cycle progression or asymmetric divisions.

APC2 and the Cadherin–Catenin Complex in the Larval Brain

The larval brain provides an opportunity to examine potential roles for APC proteins in asymmetric cell divisions. The embryonic neuroblasts in *Drosophila* are one of the best-characterized examples of this process, with many proteins required for asymmetric divisions identified (reviewed in Jan and Jan, 2001). Some of these are widely used in different asymmetric divisions in the fly. The process that triggers asymmetry can differ from cell to cell, however, with apical–basal cues used in embryonic neuroblasts (reviewed in Jan and Jan, 2001), adherens junction proteins helping orient the asymmetric divisions of certain adult sense organ precursors (Le Borgne *et al.,* 2002), and Fz signaling orienting the division in other adult sense organ precursors (Gho and Schweisguth, 1998).

Larval neuroblasts are less well characterized than their embryonic progenitors. We thus examined APC2 localization in these cells through the cell cycle, and compared its localization with those of proteins involved in embryonic asymmetric divisions. APC2 has a dynamic localization. Its asymmetry is strongest during interphase, when most asymmetric proteins are either not present or not localized (although we saw weak asymmetry of Insc during interphase, differing from what occurs in embryos). The APC2 crescent diminishes as the cell enters metaphase, but remains asymmetric throughout mitosis. As cytokinesis commences, APC2 localizes very strongly to the cleavage furrow, continuing to mark the division site after cytokinesis is complete. The APC2 crescent overlaps those of Pros, Mira, and is complementary to those of Insc and Baz.

The striking asymmetric localization of APC2 in neuroblasts prompted us to examine its role there. As neither single mutant has an effect on brain development, if there is a role for APC proteins in asymmetric divisions, both APC family members must be able to carry it out. We have several hypotheses to explain the asymmetric APC2 localization. Our favorite hypothesis stems from the observation that the interphase crescent of APC2 overlaps a similar crescent formed by the cadherin–catenin complex. This prompted us to consider the relationship between the neuroblast, its GMC daughters, and the ganglion cells and neurons derived from them. In the central brain, GMCs

remain tightly associated with their neuroblast mother, an event potentially mediated by cadherin-based cell–cell adhesion. Our APC2–GFP data suggest that ganglion cell and neuronal progeny also remain in the immediate vicinity, and that each group of neurons so formed sends out axons that join to form a common nerve. These nerves express DE–cadherin, Arm, and both APCs. One possible hypothesis to explain these data is that the daughters of a single neuroblast form a structural unit, as a part of the larger scale brain architecture. If these units are functional entities, maintaining the association of the neuroblast and its daughters and granddaughters may be important. The cadherin–catenin system could mediate selective adhesion between these cells, and APC2/APC1 could work with them in adhesion, as they do in the ovary (Townsley and Bienz, 2000; Hamada and Bienz, 2002).

It is also possible that APC2/APC1 and the cadherin–catenin system work together to orient the plane of division of the neuroblast, as the cadherin–catenin complex does in the peripheral nervous system (Le Borgne *et al.,* 2002). Our data suggest that newborn GMC daughters are not positioned randomly, but instead are born adjacent to the cluster of previous GMCs. This division pattern would help maintain a compact cluster of daughters and granddaughters. Further experiments are needed to test this hypothesis. First, we will need to generate mosaic brains in which small groups of cells lack cadherin or catenin function. Second, we will need to get around the early role for APC proteins in brain development by generating clones of *APC2 APC1* double mutant cells.

An alternate possibility is that APC2 and APC1 work independently of the cadherin–catenin system to mediate asymmetric division, helping to position the spindle, perhaps by mechanisms analogous to the role APC2 appears to play in spindle anchoring in the early syncytial fly embryo. However, if such a role exists, it must act in two different modes, allowing some neuroblasts to point their spindles at the center of the APC2 crescent and others to point one spindle pole toward the edge of the crescent, the two patterns we observe *in vivo*. Finally, it is possible that asymmetric localization of APC2 is not critical in the asymmetric divisions at all; instead, the asymmetry may reflect the fact that APC2 interacts with other asymmetrically localized proteins, such as actin or the catenins.

ACKNOWLEDGMENTS

and M.P. was supported in part by a CDA from the U.S. Army Breast Cancer Research Program.

REFERENCES

Ahmed, Y., Hayashi, S., Levine, A., and Wieschaus, E. (1998). Regulation of armadillo by a *Drosophila* APC inhibits neuronal apoptosis during retinal development. *Cell* **93,** 1171–1182.

Ahmed, Y., Nouri, A., and Wieschaus, E. (2002). Drosophila Apc1 and Apc2 regulate Wingless transduction throughout development. *Development* **129,** 1751–1762.

Ceron, J., Gonzalez, C., and Tejedor, F. J. (2001). Patterns of cell division and expression of asymmetric cell fate determinants in postembryonic neuroblast lineages of Drosophila. *Dev. Biol.* **230,** 125–138.

Datta, S. (1995). Control of proliferation activation in quiescent neuroblasts of the Drosophila central nervous system. *Development* **121,** 1173–1182.

Datta, S. (1999). Activation of neuroblast proliferation in explant culture of the Drosophila larval CNS. *Brain Res.* **818,** 77–83.

Day, C. L., and Alber, T. (2000). Crystal structure of the amino-terminal coiled-coil domain of the APC tumor suppressor. *J. Mol. Biol.* **301,** 147–156.

Fodde, R., Kuipers, J., Rosenberg, C., Smits, R., Kielman, M., Gaspar, C., van Es, J. H., Breukel, C., Wiegant, J., Giles, R. H., and Clevers, H. (2001). Mutations in the APC tumour suppressor gene cause chromosomal instability. *Nat. Cell Biol.* **3,** 433–438.

Foe, V. E., Odell, G. M., and Edgar, B. A. (1993). Mitosis and morphogenesis in the *Drosophila* embryo: Point and counterpoint. In "The Development of *Drosophila* " (M. Bate and A. Martinez-Arias, Eds.), Vol. I, pp. 149–300. Cold Spring Harbor Laboratory Press, Cold Spring Harbor, NY.

Gho, M., and Schweisguth, F. (1998). Frizzled signalling controls orientation of asymmetric sense organ precursor cell divisions in *Drosophila. Nature* **393,** 178–181.

Groden, J., Thliveris, A., Samowitz, W., Carlson, M., Gelbart, L., Albertson, H., Josyln, G., Stevens, J., Spirio, L., Robertson, M., Sargeant, L., Krapcho, K., Wolff, E., Burt, R., Hughes, J. P., Warrington, J., McPherson, J., Wasmuth, J., Paslier, D. L., Abderrahim, H., Cohen, D., Leppert, M., and White, R. (1991). Identification and characterization of the familial adenomatous polyposis coli gene. *Cell* **66,** 589–600.

Hamada, F., Murata, Y., Nishida, A., Fujita, F., Tomoyasu, Y., Nakamura, M., Toyoshima, K., Tabata, T., Ueno, N., and Akiyama, T. (1999). Identification and characterization of E-APC, a novel Drosophila homologue of the tumour suppressor APC. *Genes Cells* **4,** 465–474.

Hamada, F., and Bienz, M. (2002). A Drosophila APC tumour suppressor homologue functions in cellular adhesion. *Nat. Cell Biol.* **4,** 208–213.

Hayashi, S., Rubinfeld, B., Souza, B., Polakis, P., Wieschaus, E., and Levine, A. (1997). A *Drosophila* homolog of the tumor suppressor gene adenomatous polyposis coli down-regulates β-catenin but its zygotic expression is not essential for the regulation of Armadillo. *Proc. Natl. Acad. Sci. USA* **94,** 242–247.

Ito, K., and Hotta, Y. (1992). Proliferation pattern of postembryonic neuroblasts in the brain of *Drosophila melanogaster. Dev. Biol.* **149,** 134–148.

Jan, Y. N., and Jan, L. Y. (2001). Asymmetric cell division in the Drosophila nervous system. *Nat. Rev. Neurosci.* **2,** 772–779.

Kaplan, K. B., Burds, A. A., Swedlow, J. R., Bekir, S. S., Sorger, P. K., and Nathke, I. S. (2001). A role for the Adenomatous Polyposis Coli protein in chromosome segregation. *Nat. Cell Biol.* **3,** 429–432.

Le Borgne, R., Bellaiche, Y., and Schweisguth, F. (2002). Drosophila E-cadherin regulates the orientation of asymmetric cell division in the sensory organ lineage. *Curr. Biol.* **12,** 95–104.

McCartney, B. M., Dierick, H. A., Kirkpatrick, C., Moline, M. M., Baas, A., Peifer, M., and Bejsovec, A. (1999). *Drosophila* APC2 is a cytoskeletally-associated protein that regulates Wingless signaling in the embryonic epidermis. *J. Cell Biol.* **146,** 1303–1318.

McCartney, B. M., McEwen, D. G., Grevengoed, E., Maddox, P., Bejsovec, A., and Peifer, M. (2001). *Drosophila* APC2 and Armadillo participate in tethering mitotic spindles to cortical actin. *Nat. Cell Biol.* **3,** 933–938.

McEwen, D. G., and Peifer, M. (2000). Wnt signaling: Moving in a new direction. *Curr. Biol.* **10,** R562–R564.

Mimori-Kiyosue, Y., Shiina, N., and Tsukita, S. (2000). Adenomatous polyposis coli (APC) protein moves along microtubules and concentrates at their growing ends in epithelial cells. *J. Cell Biol.* **148,** 505–518.

Munemitsu, S., Souza, B., Müller, O., Albert, I., Rubinfeld, B., and Polakis, P. (1994). The APC gene product associates with microtubules *in vivo* and promotes their assembly *in vitro. Cancer Res.* **54,** 3676–3681.

Nakagawa, H., Murata, Y., Koyama, K., Fujiyama, A., Miyoshi, Y., Monden, M., Akiyama, T., and Nakamura, Y. (1998). Identification of a brain-specific APC homologue, APCL, and its interaction with beta-catenin. *Cancer Res.* **58,** 5176–5181.

Näthke, I. S., Adams, C. L., Polakis, P., Sellin, J. H., and Nelson, W. J. (1996). The Adenomatous Polyposis Coli (APC) tumor suppressor protein localizes to plasma membrane sites involved in active cell migration. *J. Cell Biol.* **134,** 165–180.

Ohshiro, T., Yagami, T., Zhang, C., and Matsuzaki, F. (2000). Role of cortical tumour-suppressor proteins in asymmetric division of Drosophila neuroblast. *Nature* **408,** 593–596.

Pai, L.-M., Orsulic, S., Bejsovec, A., and Peifer, M. (1997). Negative regulation of Armadillo, a Wingless effector in *Drosophila. Development* **124,** 2255–2266.

Parmentier, M. L., Woods, D., Greig, S., Phan, P. G., Radovic, A., Bryant, P., and O'Kane, C. J. (2000). Rapsynoid/Partner of inscuteable controls asymmetric division of larval neuroblasts in drosophila. *J. Neurosci.* **20,** RC84.

Polakis, P. (2000). Wnt signaling and cancer. *Genes Dev.* **14,** 1837–1851.

Rocheleau, C. E., Downs, W. D., Lin, R., Wittmann, C., Bei, Y., Cha, Y.-H., Ali, M., Priess, J. R., and Mello, C. C. (1997). Wnt signaling and an APC-related gene specify endoderm in early *C. elegans* embryos. *Cell* **90,** 707–716.

Schlesinger, A., Shelton, C. A., Maloof, J. N., Meneghini, M., and Bowerman, B. (1999). Wnt pathway components orient a mitotic spindle in the early *C. elegans* embryo without requiring gene transcription in the responding cell. *Genes Dev.* **13,** 2028–2038.

Smith, K. J., Levy, D. B., Maupin, P., Pollard, T. D., Vogelstein, B., and Kinzler, K. W. (1994). Wild-type but not mutant APC associates with the microtubule cytoskeleton. *Cancer Res.* **54,** 3672–3675.

Thorpe, C. J., Schlesinger, A., Carter, J. C., and Bowerman, B. (1997). Wnt signaling polarizes an early *C. elegans* blastomere to distinguish endoderm from mesoderm. *Cell* **90,** 695–705.

Townsley, F. M., and Bienz, M. (2000). Actin-dependent membrane association of a Drosophila epithelial APC protein and its effect on junctional armadillo. *Curr. Biol.* **10,** 1339–1348.

van Es, J. H., Kirkpatrick, C., van de Wetering, M., Molenaar, M., Miles, A., Kuipers, J., Destrée, O., Peifer, M., and Clevers, H. (1999). Identification of APC2, a homologue of the adenomatous polyposis coli tumour suppressor. *Curr. Biol.* **9,** 105–108.

Yu, X., and Bienz, M. (1999). Ubiquitous expression of a Drosophila adenomatous polyposis coli homolog and its localization in cortical actin caps. *Mech. Dev.* **84,** 69–73.

Yu, X., Waltzer, L., and Bienz, M. (1999). A new Drosophila APC homologue associated with adhesive zones of epithelial cells. *Nat. Cell Biol.* **1,** 144–151.

Zumbrunn, J., Kinoshita, K., Hyman, A. A., and Näthke, I. S. (2001). Binding of the adenomatous polyposis coli protein to microtubules increases microtubule stability and is regulated by GSK3 beta phosphorylation. *Curr. Biol.* **11,** 44–49.